Eur. Phys. J. C (2022) 82:1050
https://doi.org/10.1140/epjc/s10052-022-10980-z

THE EUROPEAN PHYSICAL JOURNAL C

Regular Article - Theoretical Physics

Odd entanglement entropy in Galilean conformal field theories and flat holography

Jaydeep Kumar Basak[a], **Himanshu Chourasiya**[b], **Vinayak Raj**[c], **Gautam Sengupta**[d]

Department of Physics, Indian Institute of Technology, Kanpur 208016, India

Received: 18 September 2022 / Accepted: 29 October 2022 / Published online: 20 November 2022

Abstract The odd entanglement entropy (OEE) for bipartite states in a class of (1+1)-dimensional Galilean conformal field theories ($GCFT_{1+1}$) is obtained through an appropriate replica technique. In this context our results are compared with the entanglement wedge cross section (EWCS) for (2 + 1)-dimensional asymptotically flat geometries dual to the $GCFT_{1+1}$ in the framework of flat holography. We find that our results are consistent with the duality of the difference between the odd entanglement entropy and the entanglement entropy of bipartite states, with the bulk EWCS for flat holographic scenarios.

Contents

1 Introduction 1
2 OEE in conformal field theories 3
2.1 Odd entanglement entropy 3
2.1.1 OEE in holographic CFT_{1+1} 3
2.2 OEE for two disjoint intervals 3
2.2.1 Two disjoint intervals at zero temperature 4
2.2.2 Two disjoint intervals in a finite size system 4
2.2.3 Two disjoint intervals at a finite temperature 4
2.3 OEE for adjacent intervals 5
2.3.1 Adjacent intervals at zero temperature . . 5
2.3.2 Adjacent intervals in a finite size system . 5
2.3.3 Adjacent intervals at a finite temperature . 6
2.4 OEE for a single interval 6
2.4.1 Single interval at zero temperature 6
2.4.2 Single interval in a finite size system . . . 7
2.4.3 Single interval at a finite temperature . . 7
3 OEE in Galilean conformal field theories 8
3.1 Review of $GCFT_{1+1}$ 8
3.2 OEE for two disjoint intervals 9
3.2.1 Monodromy of $\mathcal{M}$ 9
3.2.2 Monodromy of $\mathcal{L}$ 10
3.2.3 Two disjoint intervals at zero temperature 11
3.2.4 Two disjoint intervals in a finite size system 11
3.2.5 Two disjoint intervals at a finite temperature 12
3.3 OEE for adjacent intervals 12
3.3.1 Adjacent intervals at zero temperature . . 12
3.3.2 Adjacent intervals in a finite size system . 13
3.3.3 Adjacent intervals at a finite temperature . 13
3.4 OEE for a single interval 14
3.4.1 Single interval at zero temperature 14
3.4.2 Single interval in a finite size system . . . 14
3.4.3 Single interval at a finite temperature . . 15
4 Summary and conclusions 16
Appendix A: Limiting analysis 17
References 18

[a] e-mail: jaydeep@iitk.ac.in
[b] e-mail: chim@iitk.ac.in
[c] e-mail: vraj@iitk.ac.in
[d] e-mail: sengupta@iitk.ac.in (corresponding author)

1 Introduction

Characterization of quantum entanglement has emerged as a central issue for the investigation of diverse phenomena from condensed matter physics to issues of quantum gravity. In quantum information theory the entanglement entropy (EE) defined as the von Neumann entropy of the reduced density matrix appropriately characterizes the entanglement for bipartite pure states. Although this measure is relatively simple to compute for quantum systems with finite number of degrees of freedom it is usually intractable for extended quantum many body systems. Remarkably the entanglement entropy for bipartite states in (1 + 1)-dimensional conformal field theories (CFT_{1+1}s) could be obtained through a replica technique described in [1–3]. For bipartite mixed

states however the entanglement entropy receives contributions from irrelevant classical and quantum correlations and is hence an unsuitable entanglement measure for such states. Several mixed state entanglement and correlation measures have been proposed in quantum information theory although some of these involve optimization over local operations and classical communication (LOCC) protocols and are hence not easily computable. Some of these computable measures described in the literature include the entanglement negativity [4,5] and the reflected entropy [6,7]. Another novel computable measure for characterizing mixed state entanglement termed as the *odd entanglement entropy* (OEE) has been recently proposed in [8]. The OEE may be loosely interpreted as the von Neumann entropy of the partially transposed reduced density matrix for the subsystem under consideration.[1] The authors in [8] also obtained the OEE for the bipartite mixed state of two disjoint intervals in a CFT_{1+1} through an appropriate replica technique. Furthermore it has been shown in [8] that the holographic dual of the difference between the OEE and the EE is described by the bulk entanglement wedge cross section (EWCS) for the bipartite state in question.[2] It should also be noted here that the bulk EWCS has also been proposed as a holographic dual for several other correlation measures, for example the entanglement of purification [15], the reflected entropy [6,16] and the balanced partial entanglement [17].

On a separate note in the past a class of $(1+1)$-dimensional Galilean conformal field theories ($GCFT_{1+1}$s) was described in [18–20] utilizing an İnönü-Wigner contraction of the symmetry algebra for relativistic CFT_{1+1}s. Interestingly the EE for bipartite states in these $GCFT_{1+1}$s could be also computed through an appropriate replica technique described in [21]. In subsequent works, the authors in [22–25] established a holographic construction to obtain the EE in the context of flat space holography [26,27].

As described earlier, the EE fails to be a viable entanglement measure for bipartite mixed states. In this context, the issue of characterizing mixed state entanglement for bipartite states of these $GCFT_{1+1}$s assumes a critical significance. Addressing this issue, in [28] the authors had obtained the entanglement negativity for bipartite states through a replica technique. A holographic characterization of the entanglement negativity in the flat holographic framework was also recently described in [29]. The authors utilized the algebraic sums of the lengths of extremal curves for the dual bulk asymptotically flat geometries, homologous to certain combinations of the intervals relevant to the mixed state configuration in the $GCFT_{1+1}$. These constructions were motivated by earlier constructions in the literature for the usual AdS_3/CFT_2 scenario [30–32]. Furthermore the authors in [33] obtained the bulk EWCS for bipartite states in dual $GCFT_{1+1}$s through a novel geometric construction in the context of flat holography. Recently, the holographic duality between the bulk EWCS and the balanced partial entanglement [17] was investigated and verified in [34,35]. Also the authors in [36] obtained the reflected entropy for bipartite states in $GCFT_{1+1}$s and compared their results with the EWCS to verify the duality between the EWCS and the reflected entropy described in [6] (see also [37]).

The above developments naturally lead to the interesting issue of the computation for the OEE of bipartite states in $GCFT_{1+1}$ dual to bulk asymptotically flat geometries and explicitly verify the holographic duality of the bulk EWCS with the difference between the OEE and the EE in the context of flat holography. In this article we address this significant issue and construct an appropriate replica technique to compute the OEE for bipartite states in $GCFT_{1+1}$s. To this end we first obtain the OEE for bipartite pure and mixed states in CFT_{1+1}s which are missing in the literature. Subsequently, using a replica technique, we obtain the OEE for bipartite states involving a single, two adjacent and two disjoint intervals in $GCFT_{1+1}$s at zero and finite temperatures and for finite sized systems. For the case of the two disjoint intervals we implement a geometric monodromy analysis [38] for the corresponding four point twist field correlator in the $GCFT_{1+1}$ to obtain the relevant dominant Galilean conformal block in the large central charge limit. Furthermore we compare our results to the bulk EWCS computed in [33] and explicitly verify the holographic duality with the difference between the OEE and the EE in flat holographic scenarios.

The rest of the article is organized as follows. In Sect. 2 we describe the OEE and briefly review the corresponding replica technique for bipartite states in the context of the usual relativistic CFT_{1+1}. We also utilize this replica technique to compute the OEE for certain bipartite states at zero and finite temperatures and in finite sized systems described by CFT_{1+1}s which were missing in the literature. Subsequently, in Sect. 3, after a brief review of the $(1+1)$-dimensional non-relativistic Galilean conformal field theories, we establish a replica technique to compute the OEE for various bipartite states in $GCFT_{1+1}$s and compare our results with the bulk EWCS. In Sect. 4 we present a summary of our work and the conclusions. Finally in Appendix A we provide a limiting analysis where we show that our result of the OEE for the bipartite mixed state of two disjoint interval is consistent with the appropriate non-relativistic limit of the corresponding CFT_{1+1} result.

[1] The OEE is not exactly the von Neumann entropy as the (partially transposed) density matrix utilized does not correspond to any physical state and may have negative eigenvalues.

[2] See [9–14] for further developments on the OEE.

2 OEE in conformal field theories

2.1 Odd entanglement entropy

We begin with a brief review of the odd entanglement entropy (OEE), introduced in [8] as a correlation measures between the two subsystems of a bipartite mixed state. It can roughly be described as the von Neumann entropy of the partially transposed reduced density matrix of the given subsystem (cf. footnote 1). In this context, one starts with a tripartite pure state composed of the subsystems A_1, A_2 and B. Subsequently the subsystem B is traced out to obtain the bipartite mixed state for the subsystem $A = A_1 \cup A_2$ with the reduced density matrix $\rho_{A_1A_2}$ defined on the Hilbert space $\mathcal{H} = \mathcal{H}_{A_1} \otimes \mathcal{H}_{A_2}$. The partial transposition of the reduced density matrix $\rho_{A_1A_2}$ with respect to the subsystem A_2 is defined as

$$\langle e_i^{(1)} e_j^{(2)} | \rho_{A_1A_2}^{T_{A_2}} | e_k^{(1)} e_l^{(2)} \rangle = \langle e_i^{(1)} e_l^{(2)} | \rho_{A_1A_2} | e_k^{(1)} e_j^{(2)} \rangle, \quad (2.1)$$

where $|e_i^{(1)}\rangle$ and $|e_j^{(2)}\rangle$ are the bases for the Hilbert spaces $\mathcal{H}_{A_1}$ and $\mathcal{H}_{A_2}$ respectively. Further we define the Rényi generalization of the OEE for the partially transposed density matrix as follows

$$S_o^{(n_o)}(A_1 : A_2) = \frac{1}{1-n_o} \log \left[\mathrm{Tr}_{\mathcal{H}} (\rho_{A_1A_2}^{T_{A_2}})^{n_0} \right] \quad (2.2)$$

where n_o is an odd integer.[3] The odd entanglement entropy S_o for the given mixed state $\rho_{A_1A_2}$ may finally be obtained through the analytic continuation of the odd integer $n_o \to 1$ in the above expression as follows[4] [8]

$$S_o(A_1 : A_2) = \lim_{n_o \to 1} [S_o^{(n_o)}(A_1 : A_2)]. \quad (2.3)$$

In [9], the authors numerically confirmed the following quantum information properties which ensures that the OEE is a well-defined bipartite mixed state measure:

- $S_o(A : B) \geq 0$ (positive semi-definite)
- $S_o(A : B_1B_2) \geq S_o(A : B_1)$ (monotonic)
- $S_o(A : B_1B_2) \leq S_o(A : B_1) + S_o(A : B_2)$ (polygamy relation)
- $S_o(A_1A_2 : B_1B_2) \geq S_o(A_1 : B_1) + S_o(A_2 : B_2)$ (breaking of strong super additivity).

However, a general analytic proof of these properties remain an open issue.

[3] The partially transposed density matrix raised to an even power leads to another mixed state entanglement measure termed the entanglement negativity [4].

[4] The author in [8], instead used the Tsallis entropy to obtain the OEE. However note that, in the replica limit $n_o \to 1$ both the Rényi generalization of the OEE in Eq. (2.2) and the Tsallis entropy considered in [8] matches and gives the same expression for the OEE.

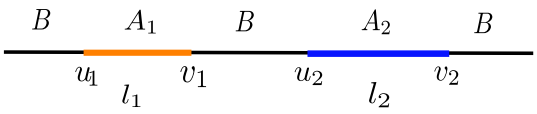

Fig. 1 Two disjoint intervals A_1 and A_2

2.1.1 OEE in holographic CFT_{1+1}

In this subsection, we review the replica technique utilized for the computation of the OEE in $(1+1)$-dimensional conformal field theories (CFT_{1+1}s) as described in [8]. For the CFT_{1+1}s, the trace $\mathrm{Tr}_{\mathcal{H}}(\rho_{A_1A_2}^{T_{A_2}})^{n_o}$ in Eq. (2.2) may be expressed as a twist field correlator corresponding to the mixed state in question. We consider a generic tripartite pure state in a CFT_{1+1} which is described by the intervals $A_1 = [u_1, v_1]$, $A_2 = [u_2, v_2]$ and $B = (A_1 \cup A_2)^c$ as shown in Fig. 1. For the bipartite mixed state of $A_1 \cup A_2$ obtained by tracing out the degrees of freedom corresponding to the subsystem B, the trace $\mathrm{Tr}_{\mathcal{H}}(\rho_{A_1A_2}^{T_{A_2}})^{n_o}$ may be expressed as a four-point twist field correlator on the complex plane as follows [8,39]

$$\mathrm{Tr}_{\mathcal{H}}(\rho_{A_1A_2}^{T_{A_2}})^{n_o} = \left\langle \mathcal{T}_{n_o}(u_1) \bar{\mathcal{T}}_{n_o}(v_1) \bar{\mathcal{T}}_{n_o}(u_2) \mathcal{T}_{n_o}(v_2) \right\rangle. \quad (2.4)$$

Here $\mathcal{T}_{n_o}$ and $\bar{\mathcal{T}}_{n_o}$ are the twist and anti-twist field operators in CFT_{1+1} respectively with the following weights,

$$h_{\mathcal{T}_{n_o}} = \bar{h}_{\bar{\mathcal{T}}_{n_o}} = \frac{c}{24} \left(n_o - \frac{1}{n_o} \right), \quad (2.5)$$

where c is the central charge. The four point twist correlator in Eq. (2.4) was utilized in [8] to obtain the OEE for the bipartite mixed state of two disjoint intervals in a CFT_{1+1} at zero temperature. In this article, we further utilize the above replica technique to obtain the OEE for the bipartite states of two disjoint intervals at a finite temperature and for a finite sized system. We also obtain the OEE for two adjacent and a single interval at zero and finite temperatures and for a finite sized system in CFT_{1+1}s.

In context of the AdS_3/CFT_2 correspondence, the authors in [8] have also proposed a holographic duality for the difference of the OEE and the EE in terms of the bulk minimal entanglement wedge cross section (EWCS) corresponding to the bipartite state under consideration as follows

$$S_o(A_1 : A_2) - S(A_1 \cup A_2) = E_W(A_1 : A_2), \quad (2.6)$$

where $S(A_1 \cup A_2)$ denotes the EE and $E_W(A_1 : A_2)$ denotes the minimal EWCS for the subsystem $A_1 \cup A_2$.

2.2 OEE for two disjoint intervals

In the following subsections we first review the OEE for two disjoint intervals at zero temperature as computed in [8]. Subsequently we compute the OEE for the bipartite mixed

state configuration of two disjoint intervals in a finite sized system and at a finite temperature using the replica technique described earlier.

2.2.1 Two disjoint intervals at zero temperature

For this case, consider the mixed state configuration of two disjoint intervals $A_1 \equiv [u_1, v_1]$ and $A_2 \equiv [u_2, v_2]$ in the vacuum state of the CFT_{1+1}. This configuration is described by the four point twist correlator given in Eq. (2.4) which may be expanded in terms of the conformal blocks in the t-channel as [8]

$$\frac{\left\langle \mathcal{T}_n(u_1)\bar{\mathcal{T}}_n(v_1)\bar{\mathcal{T}}_n(u_2)\mathcal{T}_n(v_2)\right\rangle}{(|u_1-v_2||v_1-u_2|)^{(-\frac{c}{6}[\frac{n^2-1}{n}])}} = \sum_p b_p\, \mathcal{F}(c, h_{\mathcal{T}_n}, h_p, 1-x)\, \bar{\mathcal{F}}(c, \bar{h}_{\bar{\mathcal{T}}_n}, \bar{h}_p, 1-\bar{x}), \tag{2.7}$$

where $x = \frac{|u_1-v_1||u_2-v_2|}{|u_1-u_2||v_1-v_2|}$ is the cross ratio, b_p is the OPE coefficient[5] and $\mathcal{F}$ and $\bar{\mathcal{F}}$ are the Virasoro conformal blocks corresponding to the exchange of the primary operator with the dimension h_p. In the t-channel, the dominant contribution arises from the twist field operator $\mathcal{T}^2_{n_o}$ with the weight $h^{(2)}_{\mathcal{T}_{n_o}} = h_{\mathcal{T}_{n_o}}$. The conformal block for this case may be expressed as [8,40]

$$\log \mathcal{F}(c, h_{\mathcal{T}_{n_o}}, h^{(2)}_{\mathcal{T}_{n_o}}, 1-x) = -h_{\mathcal{T}^{(2)}_{n_o}} \log\left[\frac{1+\sqrt{x}}{1-\sqrt{x}}\right]. \tag{2.8}$$

Using the above expression and Eqs. (2.7) and (2.3), one may obtain the OEE for the mixed state of two disjoint intervals in the CFT_{1+1} as follows [8]

$$S_o(A_1 : A_2) = S(A_1 \cup A_2) + \frac{c}{6}\log\left[\frac{1+\sqrt{x}}{1-\sqrt{x}}\right] + \cdots, \tag{2.9}$$

where ellipsis denote subsequent terms which are subleading in the large central charge limit. The first term in the above expression denotes the EE for the subsystem $A_1 \cup A_2$ given as

$$S(A_1 \cup A_2) = \frac{c}{3}\log\left(\frac{|u_1-v_2|}{a}\right) + \frac{c}{3}\log\left(\frac{|v_1-u_2|}{a}\right) + \cdots, \tag{2.10}$$

where a is a UV cut off of the CFT_{1+1}. It is straightforward to check that in the large central charge limit, Eq. (2.9) satisfies the duality in Eq. (2.6) as the second term matches exactly with the corresponding EWCS obtained in [15].

[5] The contribution due to the OPE coefficient is negligible in the large central charge limit as it is independent of the position of the primary operators [8].

2.2.2 Two disjoint intervals in a finite size system

For this case, we consider the mixed state configuration of two disjoint intervals A_1 and A_2 of lengths l_1 and l_2 respectively, in a CFT_{1+1} described on a cylinder with circumference L. To obtain the OEE for the given mixed state under consideration, it is necessary to compute the corresponding four point twist correlator in Eq. (2.4) on the cylinder. This may be done by utilizing the following conformal map which maps the complex plane to a cylinder [3,39]

$$z \to \omega = \frac{iL}{2\pi}\log z, \tag{2.11}$$

where z describe the coordinates on the complex plane and w describe the coordinates on the cylinder. Under this conformal map, the cross-ratio modifies as

$$\tilde{x} = \frac{\sin\left(\frac{\pi l_1}{L}\right)\sin\left(\frac{\pi l_2}{L}\right)}{\sin\left(\frac{\pi(l_1+l_s)}{L}\right)\sin\left(\frac{\pi(l_2+l_s)}{L}\right)}, \tag{2.12}$$

where l_s represents the length of the region sandwiched between the two intervals A_1 and A_2. Now, utilizing Eqs. (2.9), (2.11) and (2.12), we may obtain the OEE for the mixed state of two disjoint intervals in question as

$$S_o(A_1 : A_2) = \frac{c}{3}\log\left(\frac{L}{\pi a}\sin\frac{\pi(l_1+l_2+l_s)}{L}\right) + \frac{c}{3}\log\left(\frac{L}{\pi a}\sin\frac{\pi l_s}{L}\right) + \frac{c}{6}\log\left[\frac{1+\sqrt{\tilde{x}}}{1-\sqrt{\tilde{x}}}\right] + \cdots, \tag{2.13}$$

where a is a UV cut-off. Note that the first two terms in the above expression denote the EE $S(A_1 \cup A_2)$ for the subsystem $A_1 \cup A_2$. The corresponding bulk EWCS for this bipartite state may be obtained easily by utilizing Eq. (2.11). On computing the bulk EWCS we observe that it matches exactly with the last term in the above expression for the OEE. This provides substantiation to our computations as Eq. (2.13) is consistent with the holographic duality described in Eq. (2.6).

2.2.3 Two disjoint intervals at a finite temperature

We now turn our attention to the mixed state configuration of two disjoint intervals at a finite temperature. To this end, we consider two disjoint intervals A_1 and A_2 of lengths l_1 and l_2 respectively, in a CFT_{1+1} at a finite temperature defined on a thermal cylinder with circumference given by the inverse temperature β. To obtain the OEE for this case, it is required to obtain the four point twist correlator in Eq. (2.4) on the

thermal cylinder. We may employ the following conformal map to transform the complex plane to the thermal cylinder [3,39]

$$z \to \omega = \frac{\beta}{2\pi} \log z, \tag{2.14}$$

where z denote the coordinates on the complex plane and w denotes the coordinates on the thermal cylinder. The CFT cross-ratio modifies under this transformation as

$$\hat{x} = \frac{\sinh\left(\frac{\pi l_1}{\beta}\right)\sinh\left(\frac{\pi l_2}{\beta}\right)}{\sinh\left(\frac{\pi(l_1+l_s)}{\beta}\right)\sinh\left(\frac{\pi(l_2+l_s)}{\beta}\right)}, \tag{2.15}$$

where, similar to the previous case, l_s is the length of the region sandwiched between the disjoint intervals A_1 and A_2. Now using Eqs. (2.14), (2.15) and (2.9) we may obtain the OEE for the mixed state of two disjoint intervals at a finite temperature as

$$\begin{aligned} S_o(A_1 : A_2) = &\frac{c}{3}\log\left(\frac{\beta}{\pi a}\sinh\frac{\pi(l_1+l_2+l_s)}{\beta}\right) \\ &+\frac{c}{3}\log\left(\frac{\beta}{\pi a}\sinh\frac{\pi l_s}{\beta}\right) \\ &+\frac{c}{6}\log\left[\frac{1+\sqrt{\hat{x}}}{1-\sqrt{\hat{x}}}\right]+\cdots. \end{aligned} \tag{2.16}$$

Again note that the first two terms correspond to the EE for the mixed state $A_1 \cup A_2$ and the last term matches exactly with the corresponding bulk EWCS obtained in [15] which is consistent with the holographic duality (2.6).

2.3 OEE for adjacent intervals

Having computed the OEE for the various bipartite state configurations of two disjoint intervals, we now turn our attention to the OEE for the mixed states described by two adjacent intervals.

2.3.1 Adjacent intervals at zero temperature

For the zero temperature case we consider two adjacent intervals $A_1 \equiv [-l_1, 0]$ and $A_2 \equiv [0, l_2]$ in the CFT_{1+1}. This configuration may be obtained by taking the limit $v_1 \to u_2$ in Eq. (2.4). The trace $\mathrm{Tr}(\rho_{A_1A_2}^{T_{A_2}})^{n_o}$ may then be obtained by the following three point twist correlator on the complex plane

$$\mathrm{Tr}(\rho_{A_1A_2}^{T_{A_2}})^{n_o} = \left\langle \mathcal{T}_{n_o}(-l_1)\bar{\mathcal{T}}_{n_o}^2(0)\mathcal{T}_{n_o}(l_2)\right\rangle. \tag{2.17}$$

Using the usual form of a three point correlator in a CFT_{1+1}, we may obtain the OEE for the mixed state in question by using Eq. (2.3) as follows

$$S_o(A_1 : A_2) = \frac{c}{6}\log\left(\frac{l_1 l_2}{a^2}\right) + \frac{c}{6}\log\left(\frac{l_1+l_2}{a}\right)+\cdots, \tag{2.18}$$

where a is again a UV cut off for the CFT_{1+1}. Note that the above expression matches exactly with the corresponding OEE computed in [9] in the context of 1-dimensional harmonic spin chain and in [14] for the gravitational path integral computation based on fixed area states.[6] We may also rewrite the above expression as follows

$$S_o(A_1 : A_2) - S(A_1 \cup A_2) = \frac{c}{6}\log\left(\frac{l_1 l_2}{a(l_1+l_2)}\right)+\cdots, \tag{2.19}$$

where $S(A_1 \cup A_2)$ denotes the EE for the corresponding mixed state $A_1 \cup A_2$ given as

$$S(A_1 \cup A_2) = \frac{c}{3}\log\left(\frac{l_1+l_2}{a}\right)+\cdots. \tag{2.20}$$

We observe here that the right-hand-side of Eq. (2.19) matches with the corresponding EWCS [41] apart from an additive constant which is contained in the OPE coefficient of the corresponding three point twist correlator in Eq. (2.17). We would also like to note here that the adjacent intervals configuration under consideration can also be obtained through an appropriate adjacent limit $v_1 \to u_2$ of the disjoint intervals configuration discussed in Sect. 2.2.1, and our results in Eqs. (2.9) and (2.18) are consistent with this limiting behaviour.

2.3.2 Adjacent intervals in a finite size system

We now proceed to the mixed state of two adjacent intervals in a finite size system. For this case we consider the bipartite configuration involving two adjacent intervals A_1 and A_2 of lengths l_1 and l_2 respectively, in a CFT_{1+1} defined on a cylinder with circumference L. We again employ the conformal transformation in Eq. (2.11), which maps the complex plane to the required cylinder of circumference L. We may now obtain the OEE for the mixed state configuration in question by using Eqs. (2.11) and (2.18) as follows

$$\begin{aligned} &S_o(A_1 : A_2) \\ &= \frac{c}{6}\log\left[\left(\frac{L}{\pi a}\right)^3 \sin\left(\frac{\pi l_1}{L}\right)\sin\left(\frac{\pi l_2}{L}\right)\right. \\ &\quad \left.\sin\left(\frac{\pi(l_1+l_2)}{L}\right)\right]+\cdots, \end{aligned} \tag{2.21}$$

where a is a UV cut-off. Again, the above result can also be obtained through the appropriate adjacent limit $v_1 \to u_2$ in

[6] Note that in [14], the OEE has been termed as the "partially transposed entropy" due to the loose interpretation of the OEE being the analogue of the EE for the partially transposed density matrix.

the disjoint intervals result given in Eq. 2.13. This serves as a yet another consistency check for our computations.

We may rewrite the above expression in the following way

$$S_o(A_1:A_2)-S(A_1\cup A_2) = \frac{c}{6}\log\left[\frac{L}{\pi a}\frac{\sin\left(\frac{\pi l_1}{L}\right)\sin\left(\frac{\pi l_2}{L}\right)}{\sin\left(\frac{\pi(l_1+l_2)}{L}\right)}\right]+\cdots, \tag{2.22}$$

where $S(A_1\cup A_2)$ is the EE for the corresponding mixed state $A_1\cup A_2$ given as

$$S(A_1\cup A_2)=\frac{c}{3}\log\left[\frac{L}{\pi a}\sin\left(\frac{\pi(l_1+l_2)}{L}\right)\right]+\cdots. \tag{2.23}$$

Similar to the Sect. 2.2.2, we obtain the corresponding bulk EWCS for this case by utilizing Eq. (2.11) and find that it matches with the right-hand-side of Eq. (2.22), modulo a constant contained in the undetermined OPE coefficient of the corresponding three point twist correlator.

2.3.3 Adjacent intervals at a finite temperature

For this case, we consider the mixed state configuration of two adjacent intervals A_1 and A_2 of lengths l_1 and l_2 respectively, in a CFT_{1+1} at a finite temperature $T=1/\beta$ defined on a thermal cylinder with circumference β. Similar to the finite size case in the previous subsection, we may compute the corresponding three point twist correlator given in Eq. (2.17) on the thermal cylinder using the conformal map in Eq. (2.14). Finally we may obtain the OEE for the two adjacent intervals at a finite temperature using Eq. (2.3) to be

$$S_o(A_1:A_2)=\frac{c}{6}\log\left[\left(\frac{\beta}{\pi a}\right)^3\sinh\left(\frac{\pi l_1}{\beta}\right)\sinh\left(\frac{\pi l_2}{\beta}\right)\times\sinh\left(\frac{\pi(l_1+l_2)}{\beta}\right)\right]+\cdots, \tag{2.24}$$

where a is a UV cut off. We again note that the present bipartite configuration under consideration may also be obtained through an appropriate adjacent limit of the disjoint intervals configuration in Sect. 2.2.3, and our result in the above expression conforms to this limiting behaviour.

We may rewrite Eq. (2.24) in the following way

$$S_o(A_1:A_2)-S(A_1\cup A_2) = \frac{c}{6}\log\left[\frac{\beta}{\pi a}\frac{\sinh\left(\frac{\pi l_1}{\beta}\right)\sinh\left(\frac{\pi l_2}{\beta}\right)}{\sinh\left(\frac{\pi(l_1+l_2)}{\beta}\right)}\right]+\cdots, \tag{2.25}$$

where $S(A_1\cup A_2)$ is the EE for the bipartite state $A_1\cup A_2$ given as

$$S(A_1\cup A_2)=\frac{c}{3}\log\left[\frac{\beta}{\pi a}\sinh\left(\frac{\pi(l_1+l_2)}{\beta}\right)\right]+\cdots. \tag{2.26}$$

Similar to the previous cases, the expression for the corresponding EWCS is not present in the literature. However we expect that the above equation is consistent with the duality (2.6) and the right-hand-side denotes the EWCS apart from the an additive constant arising from the OPE coefficient of the corresponding three point twist correlator. We again leave the explicit computation of the EWCS and the verification of our claim to future prospects.

2.4 OEE for a single interval

Having discussed the bipartite configurations involving two disjoint and adjacent intervals, we finally turn our attention to the OEE for bipartite pure and mixed states involving a single interval in CFT_{1+1}s.

2.4.1 Single interval at zero temperature

In this subsection, we consider the pure state of a single interval $A_1\equiv[u_1,v_1]$ of length $l=|u_1-v_1|$ in the CFT_{1+1}, which may be obtained through the limit $u_2\to v_1$ and $v_2\to u_1$ in Eq. (2.4). For this case $A_1\cup A_2$ describes the full system with B as a null set. In this limit the four point twist correlator in Eq. (2.4) reduces to the following two point twist correlator:

$$\mathrm{Tr}_{\mathcal{H}}(\rho_{A_1A_2}^{T_{A_2}})^{n_o}=\left\langle\mathcal{T}_{n_o}^2(u_1)\bar{\mathcal{T}}_{n_o}^2(v_1)\right\rangle. \tag{2.27}$$

Here the twist field operator $\mathcal{T}_{n_o}^2$ connects the n_o-th sheet with the (n_o+2)-th sheet and have dimensions $h^{(2)}_{\mathcal{T}_{n_o}}=h_{\mathcal{T}_{n_o}}$. As described in [39], the above two point twist correlator is different for the even and the odd exponents of the trace $\mathrm{Tr}_{\mathcal{H}}(\rho_{A_1A_2}^{T_{A_2}})^n$. For the present case where we have $n=n_o$ odd, the twist field operator $\mathcal{T}_{n_o}^2$ in the above two point twist correlator simply results in the reorganization of the n_o replica sheets but does not change the structure of the n_o-sheeted Riemann manifold[7] and hence we have the following [39]

$$\mathrm{Tr}_{\mathcal{H}}(\rho_{A_1A_2}^{T_{A_2}})^{n_o}=\left\langle\mathcal{T}_{n_o}(u_1)\bar{\mathcal{T}}_{n_o}(v_1)\right\rangle=\mathrm{Tr}_{\mathcal{H}}(\rho_{A_1})^{n_o}. \tag{2.28}$$

The OEE for the single interval in question may now be obtained using Eqs. (2.2) and (2.3) as

$$S_o(A_1:A_2)=\frac{c}{3}\log\left(\frac{|u_1-v_1|}{a}\right)+\text{const.}, \tag{2.29}$$

where a is a UV cut-off and the constant is due to the normalization of the two point twist correlator. As can be clearly seen, for the pure state configuration of the single interval in question, the OEE matches exactly with the EWCS [15]

[7] Interestingly for even integers $n=n_e$, the n_e-sheeted Riemannian manifold decouples into two independent $(n_e/2)$-sheeted Riemann surfaces.

which is identically equal to the the EE [1,3]. This is in accordance with the expectation [8] that for a pure state the OEE should reduce to the EE of the interval A and the duality in Eq. (2.6) as the entropy $S(A_1 \cup A_2)$ vanishes for the state $A_1 \cup A_2$ describing the complete system.

2.4.2 Single interval in a finite size system

In this subsection we now focus on the configuration of a single interval in a finite sized system. To this end, we consider an interval A_1 of length l with A_2 describing the rest of the system in a finite sized CFT_{1+1} of length L with periodic boundary condition. In this instance, the two point twist correlator in Eq. (2.28) is required to be computed on a cylinder of circumference L. This is done by utilizing the conformal map given in Eq. (2.11). The OEE may then be obtained for the single interval in the finite sized system through Eqs. (2.28), (2.2) and (2.3) as

$$S_o(A_1 : A_2) = \frac{c}{3} \log \left(\frac{L}{\pi a} \sin \frac{\pi l}{L} \right) + \cdots . \tag{2.30}$$

Similar to the previous case, we observe that the OEE for the single interval in question matches exactly with the corresponding EE for the interval A_1 [1,3]. This is again in accordance with the duality (2.6) as for this pure state configuration, $S(A_1 \cup A_2) = 0$ and the EWCS reduces to the EE for A_1 [15].

2.4.3 Single interval at a finite temperature

For this case, we consider a single interval $A \equiv [-l, 0]$ in a CFT_{1+1} at a finite temperature T defined on a thermal cylinder with circumference $\beta = 1/T$. As described in [42] in the context of the entanglement negativity and in [43] in the context of the reflected entropy, it is necessary to consider two large but finite auxiliary intervals $B_1 \equiv [-L, -l]$, $B_2 \equiv [0, L]$ placed on either side of the interval A in question. The OEE for the given single interval may then be obtained by utilizing the following four point twist correlator,

$$\begin{aligned} &S_o(A : B) \\ &= \lim_{L\to\infty} \lim_{n_o \to 1} \frac{1}{1-n_o} \log \\ &\quad \times \left[\left\langle \mathcal{T}_{n_o}(-L) \overline{\mathcal{T}}^2_{n_o}(-l) \mathcal{T}^2_{n_o}(0) \overline{\mathcal{T}}_{n_o}(L) \right\rangle_\beta \right], \end{aligned} \tag{2.31}$$

where the subscript β denotes that the twist correlator is being evaluated on the thermal cylinder with circumference β. Note that the bipartite limit $B \equiv B_1 \cup B_2 \to A^c$ $(L \to \infty)$ has to be applied after the replica limit $n_o \to 1$ in the above equation as described in [42]. On the complex plane, the four point twist correlator described in Eq. (2.31) can be expressed as [42]

$$\begin{aligned} &\left\langle \mathcal{T}_{n_o}(z_1) \overline{\mathcal{T}}^2_{n_o}(z_2) \mathcal{T}^2_{n_o}(z_3) \overline{\mathcal{T}}_{n_o}(z_4) \right\rangle_{\mathbb{C}} \\ &= \frac{k_{n_o}}{z_{14}^{2h_{\mathcal{T}_{n_o}}} z_{23}^{2h^{(2)}_{\mathcal{T}_{n_o}}}} \frac{\mathcal{F}_{n_o}(x)}{x^{h^{(2)}_{\mathcal{T}_{n_o}}}}, \end{aligned} \tag{2.32}$$

where k_{n_o} is a constant, $x = \frac{z_{12} z_{34}}{z_{13} z_{24}}$ is the cross ratio and $\mathcal{F}_{n_o}(x)$ is an arbitrary non universal function of the cross ratio. This non universal function in the limits $x \to 1$ and $x \to 0$ may be given as [42]

$$\mathcal{F}_{n_o}(1) = 1, \quad \mathcal{F}_{n_o}(0) = C_{n_o}, \tag{2.33}$$

where C_{n_o} is a non universal constant which depends on the full operator content of the field theory. The four point twist correlator in Eq. (2.31) on the thermal cylinder may be obtained by utilizing the transformation in Eq. (2.14). The OEE for the mixed state configuration of the single interval in question may then be obtained using Eqs. (2.2) and (2.3) as

$$\begin{aligned} S_o(A : B) = &\lim_{L\to\infty} \left[\frac{c}{3} \log \left(\frac{\beta}{\pi a} \sinh \frac{2\pi L}{\beta} \right) \right] \\ &+ \frac{c}{3} \log \left(\frac{\beta}{\pi a} \sinh \frac{\pi l}{\beta} \right) - \frac{\pi c l}{3\beta} + f\left(e^{-\frac{2\pi l}{\beta}} \right) \\ &+ \cdots , \end{aligned} \tag{2.34}$$

where a is a UV cut-off for the CFT_{1+1} and the non-universal function $f(x) = \lim_{n_o \to 1} \ln \left[\mathcal{F}_{n_o}(x) \right]$. Note that in the above expression first divergent term denotes the entanglement entropy $S(A \cup B)$ of total thermal system $A \cup B$ where the bipartite limit $B_1 \cup B_2 \to A^c$ has been taken. The finite part of the OEE may be extracted by subtracting this divergent EE as follows

$$\begin{aligned} &S_o(A : B) - S(A \cup B) \\ &= \frac{c}{3} \log \left(\frac{\beta}{\pi a} \sinh \frac{\pi l}{\beta} \right) - \frac{\pi c l}{3\beta} + f\left(e^{-\frac{2\pi l}{\beta}} \right) + \cdots . \end{aligned} \tag{2.35}$$

It is instructive to express the above equation as

$$\begin{aligned} &S_o(A : B) - S(A \cup A^c) \\ &= S(A) - S^{\text{th}}(A) + f\left(e^{-\frac{2\pi l}{\beta}} \right) + \cdots , \end{aligned} \tag{2.36}$$

where $S(A)$ in the EE of the interval A and $S^{\text{th}}(A)$ denotes the thermal entropy. We note here that the OEE evaluated in Eq. (2.35) matches exactly with the corresponding EWCS in [44] in the large central charge limit. It is also worth pointing out that our result in Eq. (2.35) matches with the corresponding expressions for the OEE obtained in certain limits of the inverse temperature β in [8]. These serve as consistency checks for our computations.

3 OEE in Galilean conformal field theories

Having discussed the computation of the OEE for various bipartite states in relativistic CFT_{1+1}s, in this section we now proceed to the analysis of the OEE in $(1+1)$-dimensional Galilean conformal field theories ($GCFT_{1+1}$s). We start with a short review of the $GCFT_{1+1}$s and subsequently compute the OEE for bipartite states involving two disjoint, two adjacent and a single interval in $GCFT_{1+1}$s.

3.1 Review of $GCFT_{1+1}$

In this subsection, we briefly review certain essential features of $GCFT_{1+1}$ as described in [18–20]. The Galilean conformal algebra (GCA_{1+1}) for $GCFT_{1+1}$s may be obtained through a parametric İnönü-Wigner contraction of the usual Virasoro algebra which involves the rescaling of the space and the time coordinates as follows

$$t \to t, \qquad x_i \to \epsilon x_i, \tag{3.1}$$

with $\epsilon \to 0$ which implies a vanishing velocity limit $v_i \sim \epsilon$. The action of a generic Galilean conformal transformation on the coordinates is equivalent to diffeomorphisms and t-dependent shifts respectively as follows

$$t \to f(t), \qquad x \to f'(t)\, x + g(t). \tag{3.2}$$

The generators of the GCA_{1+1} in the plane representation are given as [19]

$$L_n = t^{n+1}\,\partial_t + (n+1)\,t^n\, x\,\partial_x, \qquad M_n = t^{n+1}\,\partial_x. \tag{3.3}$$

The corresponding Lie algebra for the generators are then expressed as follows

$$\begin{aligned}
[L_n, L_m] &= (m-n)L_{n+m} + \frac{C_L}{12}(n^3-n)\delta_{n+m,0},\\
[L_n, M_n] &= (m-n)M_{n+m} + \frac{C_M}{12}(n^3-n)\delta_{n+m,0},\\
[M_n, M_m] &= 0,
\end{aligned} \tag{3.4}$$

where we have different central extensions for each sector involving the central charges C_L and C_M for the $GCFT_{1+1}$. The reduction of the Lorentz invariance to a Galilean invariance for the $GCFT_{1+1}$ results in two separate components for the energy-momentum tensor [38] and are given as

$$\begin{aligned}
\mathcal{M} \equiv T_{tx} &= \sum_n M_n\, t^{-n-2},\\
\mathcal{L} \equiv T_{tt} &= \sum_n \left[L_n + (n+2)\frac{x}{t}M_n\right] t^{-n-2},
\end{aligned} \tag{3.5}$$

where the GCA generators M_n and L_n are defined in Eq. (3.3). The non-relativistic Ward identities for these two components $\mathcal{M}$ and $\mathcal{L}$ are given as [38]

$$\begin{aligned}
&\langle \mathcal{M}(x,t) V_1(x_1,t_1)\dots V_n(x_n,t_n)\rangle\\
&= \sum_{i=1}^{n}\left[\frac{h_{M,i}}{(t-t_i)^2} + \frac{1}{t-t_i}\partial_{x_i}\right]\langle V_1(x_1,t_1)\dots V_n(x_n,t_n)\rangle\,,\\
&\langle \mathcal{L}(x,t) V_1(x_1,t_1)\dots V_n(x_n,t_n)\rangle\\
&= \sum_{i=1}^{n}\left[\frac{h_{L,i}}{(t-t_i)^2} - \frac{1}{t-t_i}\partial_{t_i} + \frac{2h_{M,i}(x-x_i)}{(t-t_i)^3}\right.\\
&\quad \left. + \frac{x-x_i}{(t-t_i)^2}\partial_{x_i}\right]\langle V_1(x_1,t_1)\dots V_n(x_n,t_n)\rangle\,,
\end{aligned} \tag{3.6}$$

where V_is are $GCFT_{1+1}$ primaries and $(h_{L,i},\ h_{M,i})$ are their corresponding weights.

The usual form of a two point correlator of primary fields $V_i(x_i,t_i)$ may be obtained by utilizing the Galilean conformal symmetry as follows [18]

$$\begin{aligned}
&\langle V_1(x_1,t_1)V_2(x_2,t_2)\rangle\\
&= C^{(2)}\delta_{h_{L,1}h_{L,2}}\delta_{h_{M,1}h_{M,2}}t_{12}^{-2h_{L,1}}\exp\left(-2h_{M,1}\frac{x_{12}}{t_{12}}\right),
\end{aligned} \tag{3.7}$$

where $x_{ij} = x_i - x_j, t_{ij} = t_i - t_j$ and $C^{(2)}$ is the normalization constant. In a similar manner the three point correlator of the primary fields could be expressed as [18]

$$\begin{aligned}
&\langle V_1(x_1,t_1)V_2(x_2,t_2)V_3(x_3,t_3)\rangle\\
&= C^{(3)}t_{12}^{-(h_{L,1}+h_{L,2}-h_{L,3})}\,t_{23}^{-(h_{L,2}+h_{L,3}-h_{L,1})}\\
&\quad\times t_{13}^{-(h_{L,1}+h_{L,3}-h_{L,2})}\\
&\quad\times\exp\Big[-(h_{M,1}+h_{M,2}-h_{M,3})\frac{x_{12}}{t_{12}}\\
&\quad-(h_{M,2}+h_{M,3}-h_{M,1})\frac{x_{23}}{t_{23}}\\
&\quad-(h_{M,1}+h_{M,3}-h_{M,2})\frac{x_{13}}{t_{13}}\Big],
\end{aligned} \tag{3.8}$$

where $C^{(3)}$ is the OPE coefficient. Utilizing the Galilean symmetry, one may also express the four point correlator for primary fields $V_i(x_i,t_i)$ as [18,28]

$$\begin{aligned}
&\left\langle\prod_{i=1}^{4}V_i(x_i,t_i)\right\rangle\\
&= \prod_{1\le i<j\le 4} t_{ij}^{\frac{1}{3}\sum_{k=1}^{4}h_{L,k}-h_{L,i}-h_{L,j}}\\
&\quad \mathrm{e}^{-\frac{x_{ij}}{t_{ij}}\left(\frac{1}{3}\sum_{k=1}^{4}h_{M,k}-h_{M,i}-h_{M,j}\right)}\mathcal{G}\left(T,\frac{X}{T}\right),
\end{aligned} \tag{3.9}$$

where $\mathcal{G}(T,\frac{X}{T})$ is a non universal function which depend on the specific operator content of the $GCFT_{1+1}$. The non-relativistic cross-ratios X and $\frac{X}{T}$ of the $GCFT_{1+1}$ are given as

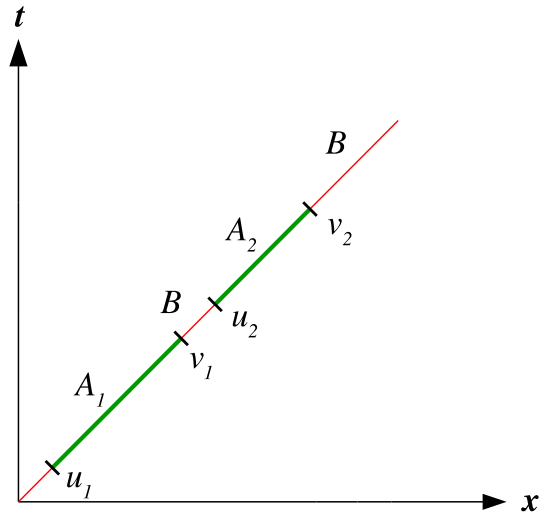

Fig. 2 Boosted intervals A_1 and A_2 in a $GCFT_{1+1}$ plane

$$T = \frac{t_{12}t_{34}}{t_{13}t_{24}}\,, \qquad \frac{X}{T} = \frac{x_{12}}{t_{12}} + \frac{x_{34}}{t_{34}} - \frac{x_{13}}{t_{13}} - \frac{x_{24}}{t_{24}}\,. \tag{3.10}$$

In the following subsections, we will now obtain the OEE for various bipartite states in $GCFT_{1+1}$s involving two disjoint, two adjacent and a single interval.

3.2 OEE for two disjoint intervals

As the $GCFT_{1+1}$ lacks the Lorentz invariance the OEE will be necessarily frame dependent and hence we need to consider Galilean boosted intervals henceforth. Similar to the relativistic case, the trace $\mathrm{Tr}_{\mathcal{H}}(\rho^{T_{A_2}}_{A_1A_2})^{n_o}$ required to obtain the OEE, can be computed through a replica technique and may be expressed as a twist correlator in the $GCFT_{1+1}$. Now let us consider the mixed state configuration of two disjoint boosted intervals $A_1 \equiv [u_1, v_1]$ and $A_2 \equiv [u_2, v_2]$ with B describing the rest of the system as shown in Fig. 2. Here $u_1 = (x_1, t_1)$, $v_1 = (x_2, t_2)$, $u_2 = (x_3, t_3)$, $v_2 = (x_4, t_4)$ are the end points of the intervals A_1 and A_2 respectively.

Similar to the case described in [28,29] where the trace of the partially transposed density matrix is raised to an even exponent, the trace $\mathrm{Tr}_{\mathcal{H}}(\rho^{T_{A_2}}_{A_1A_2})^{n_o}$ with an odd exponent n_o may be expressed as

$$\begin{aligned}&\mathrm{Tr}_{\mathcal{H}}(\rho^{T_{A_2}}_{A_1A_2})^{n_o}\\ &= \left\langle \Phi_{n_o}(u_1)\Phi_{-n_o}(v_1)\Phi_{-n_o}(u_2)\Phi_{n_o}(v_2)\right\rangle,\end{aligned} \tag{3.11}$$

where Φ_{n_o} and Φ_{-n_o} are the twist and anti-twist operators in the $GCFT_{1+1}$, respectively with the corresponding weights given as

$$h^{(1)}_L = \frac{C_L}{24}\left(n_o - \frac{1}{n_o}\right), \qquad h^{(1)}_M = \frac{C_M}{24}\left(n_o - \frac{1}{n_o}\right). \tag{3.12}$$

The four point twist correlator of Eq. (3.11) is expected to exponentiate in the large central charge limit [29], similar to the relativistic case discussed in Sect. 2.2. The dominant contribution to the four point twist correlator may thus be extracted through the geometric monodromy analysis as discussed in [24,29]. To this end, in the large C_L, C_M limit we may express the four point twist correlator in Eq. (3.11) in terms of the Galilean conformal block $\mathcal{F}_\alpha$ corresponding to the t-channel ($T \to 1$, $X \to 0$) as follows

$$\begin{aligned}&\left\langle \Phi_{n_o}(x_1,t_1)\,\Phi_{-n_o}(x_2,t_2)\,\Phi_{-n_o}(x_3,t_3)\,\Phi_{n_o}(x_4,t_4)\right\rangle\\ &= t_{14}^{-2h^{(1)}_L}\, t_{23}^{-2h^{(1)}_L}\, \exp\left[-2h^{(1)}_M \frac{x_{14}}{t_{14}} - 2h^{(1)}_M \frac{x_{23}}{t_{23}}\right]\\ &\quad \mathcal{F}_\alpha\left(T, \frac{X}{T}\right).\end{aligned} \tag{3.13}$$

The dominant conformal block $\mathcal{F}_\alpha$ is an arbitrary function of the cross-ratios X and T and depends on the full operator content of the $GCFT_{1+1}$.

In the following subsections we obtain the expression of the block $\mathcal{F}_\alpha$ in the large central charge limit by utilizing a geometric monodromy analysis [29,38] for each of the two components of the energy-momentum tensor $\mathcal{M}$ and $\mathcal{L}$ described in Eq. (3.5).

3.2.1 Monodromy of $\mathcal{M}$

In this subsection, through the geometric monodromy analysis [29,38] of the energy-momentum tensor component $\mathcal{M}$, we will obtain a partial expression for the Galilean conformal block $\mathcal{F}_\alpha$ in Eq. (3.13). In this context, utilizing the Ward identities described in Eq. (3.6), we obtain the expectation value of the $\mathcal{M}$ as

$$\mathcal{M}(u_i;(x,t)) = \sum_{i=1}^{4}\left[\frac{h_{M,i}}{(t-t_i)^2} + \frac{C_M}{6}\frac{c_i}{t-t_i}\right], \tag{3.14}$$

where u_i are the points in the $GCFT$ plane where the twist operators Φ_{n_o} are located and the auxiliary parameters c_i are given by

$$c_i = \frac{6}{C_M}\partial_{x_i}\log\left\langle \Phi_{n_o}(u_1)\,\Phi_{-n_o}(u_2)\,\Phi_{-n_o}(u_3)\,\Phi_{n_o}(u_4)\right\rangle. \tag{3.15}$$

Note that for a four point correlator, the Galilean conformal symmetry is not sufficient to fix the structure of the correlator and hence some on the auxiliary parameters c_i remain undetermined. By utilizing a Galilean transformation, we locate the twist operators at $t_1 = 0$, $t_3 = 1$, $t_4 = \infty$ and leave $t_2 = T$ free. We may express three of the auxiliary parameters in terms of the fourth by utilizing the facts that the expectation value of $\mathcal{M}$ scale as $\mathcal{M}(T;t) \sim t^{-4}$ as $t \to \infty$

and the conformal dimension $h_{M,i} \equiv h_M^{(1)}$ of the light operator Φ_{n_o} vanishes in the replica limit $n_o \to 1$. The expectation value of $\mathcal{M}$ may now be written in terms of the only unknown auxiliary parameter c_2 as follows [29]

$$\frac{6}{C_M}\mathcal{M}(T;t) = c_2\left[\frac{T-1}{t} + \frac{1}{t-T} - \frac{T}{t-1}\right]. \tag{3.16}$$

Under a generic Galilean transformation given in Eq. (3.2) the energy-momentum tensor $\mathcal{M}$ transforms as [38]

$$\mathcal{M}'(t',x') = (f')^2\mathcal{M}(t,x) + \frac{C_M}{12}\,S(f,t)\,, \tag{3.17}$$

where $S(f,t)$ is the Schwarzian derivative for the coordinate transformation $t \to f(t)$. For the ground state of the $GCFT_{1+1}$, the expectation value $\mathcal{M}(u_i;(x,t))$ vanishes on the $GCFT$ complex plane which constrains the Schwarzian derivative to have the following form

$$\frac{1}{2}\,S(f,t) = c_2\left[\frac{T-1}{t} + \frac{1}{t-T} - \frac{T}{t-1}\right]. \tag{3.18}$$

It is possible to express the above in the form of a differential equation as [29]

$$\begin{aligned} 0 &= h''(t) + \frac{1}{2}S(f,t)\,h(t) \\ &= h''(t) + \frac{6}{c_M}\mathcal{M}(T,t)\,h(t)\,, \end{aligned} \tag{3.19}$$

where $f = h_1/h_2$ with h_1 and h_2 as the two solutions of the differential equation. By utilizing the monodromy of the solutions h_1 and h_2 by circling around the light operators at $t = 1\,, T$ and using the monodromy condition for the three point twist correlator described in [29], we may obtain the auxiliary parameter c_2 as

$$c_2 = \epsilon_\alpha \frac{1}{\sqrt{T}(T-1)}\,, \tag{3.20}$$

where $\epsilon_\alpha = \frac{6}{C_M}h_{M,\alpha}$ is the rescaled weight of the corresponding conformal block $\mathcal{F}_\alpha$. We may now obtain the conformal block $\mathcal{F}_\alpha$ for the four-point function in Eq. (3.13) as

$$\begin{aligned} \mathcal{F}_\alpha &= \exp\left[\frac{C_M}{6}\int c_2\,dX\right] \\ &= \exp\left[h_{M,\alpha}\left(\frac{X}{\sqrt{T}(T-1)}\right)\right]\tilde{\mathcal{F}}(T)\,. \end{aligned} \tag{3.21}$$

Note that the complete form of the conformal block is still not known and we have an unknown function $\tilde{\mathcal{F}}(T)$ of the coordinate T in the above expression. The form of this function will be determined through the geometric monodromy analysis for the other component of the energy-momentum tensor $\mathcal{L}$ in the proceeding subsection.

3.2.2 Monodromy of $\mathcal{L}$

Similar to the Monodromy of $\mathcal{M}$ in the previous subsection, we may express the expectation value of $\mathcal{L}$ by utilizing the Galilean Ward identities in Eq. (3.6) as follows

$$\begin{aligned} \frac{6}{C_M}\mathcal{L}(u_i;(x,t)) = \sum_{i=1}^{4}\Bigg[&\frac{\delta_i}{(t-t_i)^2} - \frac{1}{t-t_i}d_i \\ &+ \frac{2\epsilon_i(x-x_i)}{(t-t_i)^3} + \frac{x-x_i}{(t-t_i)^2}c_i\Bigg], \end{aligned} \tag{3.22}$$

where $\delta_i = \frac{6}{C_M}h_{L,i}, \epsilon_i = \frac{6}{C_M}h_{M,i}$, the auxiliary parameters c_i are defined in Eq. (3.15) and the auxiliary parameters d_i are given as [38]

$$d_i = \frac{6}{C_M}\,\partial_{t_i}\log\left\langle\Phi_{n_o}(u_1)\,\Phi_{-n_o}(u_2)\,\Phi_{-n_o}(u_3)\,\Phi_{n_o}(u_4)\right\rangle. \tag{3.23}$$

By utilizing a Galilean conformal map, we locate the twist operators at $t_1 = 0, t_2 = T, t_3 = 1, t_4 = \infty$ and $x_1 = 0, x_2 = X, x_3 = 0$ and $x_4 = 0$. Again three of the four auxiliary parameters d_i may be obtained in terms of the remaining one by utilizing the scaling $\mathcal{L}(T,t) \to t^{-4}$ with $t \to \infty$. We may now rewrite Eq. (3.22) in terms of the undetermined auxiliary parameter d_2 as follows

$$\begin{aligned} &\frac{6}{C_M}\mathcal{L}(u_i;(x,t)) \\ &= -\frac{c_2X + d_2(T-1) - 2\delta_L}{t} + \frac{c_2X + d_2T - 2\delta_L}{t-1} \\ &\quad + \frac{c_1x}{t^2} + \frac{c_2(x-X)}{(t-T)^2} + \frac{c_3x}{(t-1)^2} \\ &\quad - \frac{d_2}{t-T} + \frac{2x\epsilon_L}{t^3} + \frac{\delta_L}{t^2} \\ &\quad + \frac{\delta_L}{(t-1)^2} + \frac{\delta_L}{(t-T)^2} \\ &\quad + \frac{2\epsilon_L(x-X)}{(t-T)^3} + \frac{2x\epsilon_L}{(t-1)^3}\,. \end{aligned} \tag{3.24}$$

where $\delta_L = \frac{6}{C_M}h_L^{(1)}$ and $\epsilon_L = \frac{6}{C_M}h_M^{(1)}$ are the rescaled weights of the twist operator Φ_{n_o}. We note here that the auxiliary parameters c_i appearing in the above expression are as obtained in the preceding Sect. 3.2.1.

As in [24,29], now we consider the following combination of the expectation values of the two components of the energy-momentum tensor,

$$\tilde{\mathcal{L}}(u_i;(x,t)) = \left[\mathcal{L}(u_i;(x,t)) + X\,\mathcal{M}'(u_i;(x,t))\right]. \tag{3.25}$$

By choosing an ansatz $g(t) = f'(t)Y(t)$ in the generic Galilean transformation Eq. (3.2), we get a differential equation of the following form,

$$\frac{6}{C_M}\tilde{\mathcal{L}} = -\frac{1}{2}Y''' - 2Y'\frac{6}{C_M}\mathcal{M} - Y\frac{6}{C_M}\mathcal{M}'. \tag{3.26}$$

Similar to previous subsection, through the monodromy of the solutions of the above differential equation by circling around the light operators at $t = 1, T$, we may determine the auxiliary parameter d_2 as

$$d_2 = \frac{(1-3T)X\epsilon_\alpha + 2(T-1)T\delta_\alpha}{2(T-1)^2T^{3/2}}, \tag{3.27}$$

where $\epsilon_\alpha, \delta_\alpha = \frac{6}{C_M} h_{L,\alpha}$ are the rescaled weight of $\mathcal{F}_\alpha$. The complete form of the Galilean conformal block $\mathcal{F}_\alpha$ may now be obtained by using Eqs. (3.21) and (3.23) to be

$$\mathcal{F}_\alpha = \left(\frac{1-\sqrt{T}}{1+\sqrt{T}}\right)^{h_{L,\alpha}} \exp\left[h_{M,\alpha}\left(\frac{X}{\sqrt{T}(T-1)}\right)\right]. \tag{3.28}$$

Now utilizing the above expression of the Galilean conformal block, we will obtain the OEE for the bipartite mixed states involving two disjoint intervals in $GCFT_{1+1}$s at zero and finite temperature and for a finite sized system.

3.2.3 Two disjoint intervals at zero temperature

In this subsection we compute the OEE for the bipartite mixed state of two disjoint intervals described by A_1 and A_2 in a $GCFT_{1+1}$ at zero temperature. To this end, we utilize the t-channel $T \to 1, X \to 0$ result in the large C_M, C_L limit for the Galilean conformal blocks $\mathcal{F}_\alpha$ in Eq. (3.28). In particular, the dominant conformal block for the four point twist correlator in Eq. (3.13) in the t-channel is described by the primary twist field operator $\Phi^2_{n_o}$ with the weights $h^{(2)}_L = h^{(1)}_L$ and $h^{(2)}_M = h^{(1)}_M$ where $h^{(1)}_L, h^{(1)}_M$ are as given in Eq. (3.12). Utilizing the expression for the Galilean conformal block in Eq. (3.28), we may obtain the OEE for the two disjoint intervals under consideration as follows

$$\begin{aligned} S_o(A_1:A_2) &= \frac{C_L}{6}\log\left(\frac{t_{14}t_{23}}{a^2}\right) + \frac{C_L}{12}\log\left(\frac{1+\sqrt{T}}{1-\sqrt{T}}\right) \\ &+ \frac{C_M}{6}\left(\frac{x_{14}}{t_{14}} + \frac{x_{23}}{t_{23}}\right) + \frac{C_M}{12}\frac{X}{\sqrt{T}}\left(\frac{1}{1-T}\right) \\ &+ \cdots, \end{aligned} \tag{3.29}$$

where X and T are the non relativistic cross ratios given in Eq. (3.10). The first and third term in the above expression denote the EE $S(A_1 \cup A_2)$ for the subsystem $A_1 \cup A_2$. The above expression may then be rearranged to obtain

$$\begin{aligned} S_o(A_1:A_2) - S(A_1\cup A_2) &= \frac{C_L}{12}\log\left(\frac{1+\sqrt{T}}{1-\sqrt{T}}\right) \\ &+ \frac{C_M}{12}\frac{X}{\sqrt{T}}\left(\frac{1}{1-T}\right) + \cdots, \end{aligned} \tag{3.30}$$

where the right-hand-side of the above expression matches exactly with the corresponding EWCS [33] in the context of flat holography. This verifies the duality described in Eq. (2.6) for flat holographic scenarios as well.

3.2.4 Two disjoint intervals in a finite size system

Here we compute the OEE for the bipartite configuration of two disjoint intervals in a finite sized $GCFT_{1+1}$ defined on a cylinder of circumference L. In this context we consider the two disjoint intervals to be given as $A_1 \equiv [(\xi_1, \rho_1), (\xi_2, \rho_2)]$ and $A_2 \equiv [(\xi_3, \rho_3), (\xi_4, \rho_4)]$. Similar to the relativistic case in Sect. 2.2.2, it is required to calculate the four point twist correlator in Eq. (3.13) on the given cylinder. We utilize the following conformal map to transform from the $GCFT$ complex plane to the cylinder [28,29]

$$t_i = e^{\frac{2\pi i\xi_i}{L}}, \qquad x_i = \frac{2\pi i\rho_i}{L}e^{\frac{2\pi i\xi_i}{L}}, \tag{3.31}$$

where the coordinates on the complex plane are denoted by (x_i, t_i) and the coordinates on the cylinder are denoted by (ξ_i, ρ_i). The transformation of a $GCFT_{1+1}$ primary field $\Phi(x,t)$ under this map is given as [27,28]

$$\tilde{\Phi}(\xi,\rho) = \left(\frac{L}{2\pi i}\right)^{-h_L} e^{\frac{2\pi i}{L}(\xi h_L + \rho h_M)}\Phi(x,t). \tag{3.32}$$

We may also obtain the non-relativistic cross-ratios on the cylinder by using Eq. (3.31) as

$$\tilde{T} = \frac{\sin\left(\frac{\pi\xi_{12}}{L}\right)\sin\left(\frac{\pi\xi_{34}}{L}\right)}{\sin\left(\frac{\pi\xi_{13}}{L}\right)\sin\left(\frac{\pi\xi_{24}}{L}\right)}, \tag{3.33a}$$

$$\begin{aligned} \frac{\tilde{X}}{\tilde{T}} &= \frac{\pi\rho_{12}}{L}\cot\left(\frac{\pi\xi_{12}}{L}\right) + \frac{\pi\rho_{34}}{L}\cot\left(\frac{\pi\xi_{34}}{L}\right) \\ &- \frac{\pi\rho_{13}}{L}\cot\left(\frac{\pi\xi_{13}}{L}\right) - \frac{\pi\rho_{24}}{L}\cot\left(\frac{\pi\xi_{24}}{L}\right). \end{aligned} \tag{3.33b}$$

Now utilizing Eqs. (3.31) and (3.33) in Eq. 3.29 we may obtain the OEE for the bipartite mixed state configuration of two disjoint intervals under consideration as

$$\begin{aligned} S_o(A_1:A_2) &= \frac{C_L}{6}\log\left[\left(\frac{L}{\pi a}\right)^2\sin\left(\frac{\pi\xi_{14}}{L}\right)\sin\left(\frac{\pi\xi_{23}}{L}\right)\right] \\ &+ \frac{C_L}{12}\log\left(\frac{1+\sqrt{\tilde{T}}}{1-\sqrt{\tilde{T}}}\right) + \frac{C_M}{6} \\ &\times\left[\frac{\pi\rho_{14}}{L}\cot\left(\frac{\pi\xi_{14}}{L}\right) + \frac{\pi\rho_{23}}{L}\cot\left(\frac{\pi\xi_{23}}{L}\right)\right] \\ &+ \frac{C_M}{12}\frac{\tilde{X}}{\sqrt{\tilde{T}}}\left(\frac{1}{1-\tilde{T}}\right) + \cdots, \end{aligned} \tag{3.34}$$

where again the first and the third term denote the EE $S(A_1 \cup A_2)$ for the mixed state $A_1 \cup A_2$. This allows to rewrite the above expression as follows

$$S_o(A_1:A_2) - S(A_1\cup A_2) = \frac{C_L}{12}\log\left(\frac{1+\sqrt{\tilde{T}}}{1-\sqrt{\tilde{T}}}\right)$$

$$+\frac{C_M}{12}\frac{\tilde{X}}{\sqrt{\tilde{T}}}\left(\frac{1}{1-\tilde{T}}\right)+\cdots. \tag{3.35}$$

We note here that as earlier, the right-hand-side of the above expression matches exactly with the corresponding EWCS [33] in the context of flat holography. This is once again consistent with the duality (2.6) and provides strong substantiation for our computations.

3.2.5 Two disjoint intervals at a finite temperature

Next we proceed to the computation of the OEE for two disjoint intervals in a $GCFT_{1+1}$ described on a thermal cylinder with circumference equal to the inverse temperature $\beta = 1/T$. We again employ the following conformal map to transform to the thermal cylinder [27]

$$t_i = e^{\frac{2\pi\xi_i}{\beta}}, \quad x_i = \frac{2\pi\rho_i}{\beta}e^{\frac{2\pi\xi_i}{\beta}}, \tag{3.36}$$

where (x_i, t_i) denotes the coordinates on the complex plane and (ξ_i, ρ_i) denotes the coordinates on the thermal cylinder. Again the $GCFT$ primaries transform under the above conformal map as follows [27]

$$\tilde{\Phi}(\xi,\rho) = \left(\frac{\beta}{2\pi}\right)^{-h_L^{(1)}} e^{\frac{2\pi}{\beta}(\xi h_L^{(1)}+\rho h_M^{(1)})}\Phi(x,t), \tag{3.37}$$

and the $GCFT$ cross-ratios get modified as follows

$$\hat{T} = \frac{\sinh\left(\frac{\pi\xi_{12}}{\beta}\right)\sinh\left(\frac{\pi\xi_{34}}{\beta}\right)}{\sinh\left(\frac{\pi\xi_{13}}{\beta}\right)\sinh\left(\frac{\pi\xi_{24}}{\beta}\right)}, \tag{3.38a}$$

$$\frac{\hat{X}}{\hat{T}} = \frac{\pi\rho_{12}}{\beta}\coth\left(\frac{\pi\xi_{12}}{\beta}\right)+\frac{\pi\rho_{34}}{\beta}\coth\left(\frac{\pi\xi_{34}}{\beta}\right) -\frac{\pi\rho_{13}}{\beta}\coth\left(\frac{\pi\xi_{13}}{\beta}\right)-\frac{\pi\rho_{24}}{\beta}\coth\left(\frac{\pi\xi_{24}}{\beta}\right). \tag{3.38b}$$

Utilizing Eqs. (3.36) and (3.38) in Eq. 3.29 we may now obtain the OEE for the bipartite configuration in question to be

$$\begin{aligned} S_o(A_1:A_2) = {} & \frac{C_L}{6}\log\left[\left(\frac{\beta}{\pi a}\right)^2\sinh\left(\frac{\pi\xi_{14}}{\beta}\right)\sinh\left(\frac{\pi\xi_{23}}{\beta}\right)\right] \\ & +\frac{C_L}{12}\log\left(\frac{1+\sqrt{\hat{T}}}{1-\sqrt{\hat{T}}}\right) \\ & +\frac{C_M}{6}\left[\frac{\pi\rho_{14}}{\beta}\coth\left(\frac{\pi\xi_{14}}{\beta}\right)+\frac{\pi\rho_{23}}{\beta}\coth\left(\frac{\pi\xi_{23}}{\beta}\right)\right] \\ & +\frac{C_M}{12}\frac{\hat{X}}{\sqrt{\hat{T}}}\left(\frac{1}{1-\hat{T}}\right)+\cdots. \end{aligned} \tag{3.39}$$

Similar to the previous subsections the first and the last term in the above equation denotes the EE of the mixed state $A_1 \cup A_2$ and we may express the above equation as

$$\begin{aligned} S_o(A_1:A_2) - S(A_1\cup A_2) = {} & \frac{C_L}{12}\log\left(\frac{1+\sqrt{\hat{T}}}{1-\sqrt{\hat{T}}}\right) \\ & +\frac{C_M}{12}\frac{\hat{X}}{\sqrt{\hat{T}}}\left(\frac{1}{1-\hat{T}}\right)+\cdots. \end{aligned} \tag{3.40}$$

We again note that the quantity on the right-hand-side of the above expression matches exactly with the corresponding EWCS [33] which is in accordance with the duality Eq. (2.6) in the context of flat holography. This once again provides a consistency check for our construction.

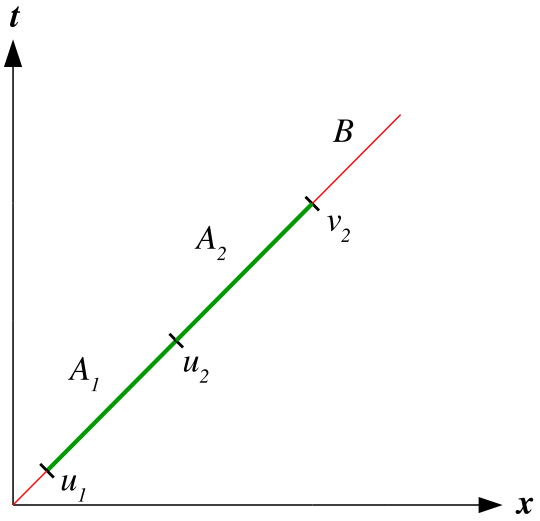

Fig. 3 Two adjacent intervals in a $GCFT_{1+1}$ plane

3.3 OEE for adjacent intervals

Having computed the OEE for bipartite configurations involving two disjoint intervals, we now turn our attention to the mixed state configurations of two adjacent intervals in $GCFT_{1+1}$s.

3.3.1 Adjacent intervals at zero temperature

For this case, we consider two adjacent intervals in a $GCFT_{1+1}$ in its ground state. In particular we consider the two adjacent intervals to be described as $A_1 \equiv [u_1, u_2]$, $A_2 \equiv [u_2, v_2]$ in $GCFT_{1+1}$ which may be obtained by taking the limit $v_1 \to u_2$ in disjoint intervals configuration considered in Sect. 3.2. In this limit, Eq. (3.11) reduces to the following three point twist correlator (Fig. 3),

$$\mathrm{Tr}(\rho_{A_1A_2}^{T_{A_2}})^{n_o} = \left\langle \Phi_{n_o}(u_1)\Phi^2_{-n_o}(u_2)\Phi_{n_o}(v_2)\right\rangle. \tag{3.41}$$

Using the usual form of a $GCFT_{1+1}$ three point correlator in Eq. (3.8) for Eq. (3.41), we may obtain the OEE for the

mixed state of two adjacent intervals under consideration as

$$S_o(A_1:A_2)=\frac{C_L}{12}\log\left(\frac{t_{12}t_{23}t_{13}}{a^3}\right)+\frac{C_M}{12}\left(\frac{x_{12}}{t_{12}}+\frac{x_{23}}{t_{23}}+\frac{x_{13}}{t_{13}}\right)+\cdots, \quad (3.42)$$

where a is the UV cut-off. The above expression may also be rewritten as

$$S_o(A_1:A_2)-S(A_1\cup A_2)=\frac{C_L}{12}\log\left(\frac{t_{12}t_{23}}{at_{13}}\right)+\frac{C_M}{12}\left(\frac{x_{12}}{t_{12}}+\frac{x_{23}}{t_{23}}-\frac{x_{13}}{t_{13}}\right)+\cdots, \quad (3.43)$$

where we have subtracted the EE for the state $A_1\cup A_2$ which is given as

$$S(A_1\cup A_2)=\frac{C_L}{6}\log\left(\frac{t_{13}}{a}\right)+\frac{C_M}{6}\left(\frac{x_{13}}{t_{13}}\right). \quad (3.44)$$

Note that we may obtain the result in Eq. (3.42) by taking an appropriate adjacent limit $(x_2,t_2)\to(x_3,t_3)$ of the corresponding disjoint intervals result in Eq. (3.29). We also observe that the expression for the difference of the OEE and the entropy in Eq. (3.43) matches with the corresponding EWCS in [33] apart from an additive constant which is contained in the undetermined OPE coefficient of the corresponding three point twist correlator in Eq. (3.41). This is in accordance with the duality in Eq. (2.6). These observations serve as consistency checks for our results.

3.3.2 Adjacent intervals in a finite size system

For this case, we consider the bipartite mixed state configuration of two adjacent intervals described by $A_1\equiv[(\xi_1,\rho_1),(\xi_2,\rho_2)]$ and $A_2\equiv[(\xi_2,\rho_2),(\xi_3,\rho_3)]$ in a finite sized $GCFT_{1+1}$ described on a cylinder of circumference L. It is again necessary here to compute the corresponding three point twist correlator on the cylinder. To this end, we employ the conformal map in Eq. (3.31) and the transformation of the $GCFT_{1+1}$ primaries given in Eq. (3.32) to obtain

$$\left\langle\Phi_{n_o}(\xi_1,\rho_1)\Phi^2_{-n_o}(\xi_2,\rho_2)\Phi_{n_o}(\xi_3,\rho_3)\right\rangle=\left(\frac{L}{2\pi i}\right)^{-2h_L^{(1)}-h_L^{(2)}}\exp\left[\frac{2\pi i}{L}\left(\xi_1h_L^{(1)}+\xi_2h_L^{(2)}+\xi_3h_L^{(1)}+\rho_1h_M^{(1)}+\rho_2h_M^{(2)}+\rho_3h_M^{(1)}\right)\right]\times\left\langle\Phi_{n_o}(u_1)\Phi^2_{-n_o}(u_2)\Phi_{n_o}(v_2)\right\rangle, \quad (3.45)$$

where the three point twist correlator on the right-hand-side is defined on the $GCFT$ complex plane. Utilizing Eqs. (3.45) and (3.8) in Eqs. (2.2) and (2.3) we may now obtain the OEE for the mixed state under consideration as follows

$$S_o(A_1:A_2)=\frac{C_L}{12}\log\left[\left(\frac{L}{\pi a}\right)^3\sin\left(\frac{\pi\xi_{12}}{L}\right)\times\sin\left(\frac{\pi\xi_{23}}{L}\right)\sin\left(\frac{\pi\xi_{13}}{L}\right)\right]+\frac{C_M}{12}\left[\frac{\pi\rho_{12}}{L}\cot\left(\frac{\pi\xi_{12}}{L}\right)+\frac{\pi\rho_{23}}{L}\cot\left(\frac{\pi\xi_{23}}{L}\right)+\frac{\pi\rho_{13}}{L}\cot\left(\frac{\pi\xi_{13}}{L}\right)\right]+\cdots. \quad (3.46)$$

It is instructive to rewrite the above result as

$$S_o(A_1:A_2)-S(A_1\cup A_2)=\frac{C_L}{12}\log\left[\frac{L}{\pi a}\frac{\sin\left(\frac{\pi\xi_{12}}{L}\right)\sin\left(\frac{\pi\xi_{23}}{L}\right)}{\sin\left(\frac{\pi\xi_{13}}{L}\right)}\right]+\frac{C_M}{12}\left[\frac{\pi\rho_{12}}{L}\cot\left(\frac{\pi\xi_{12}}{L}\right)+\frac{\pi\rho_{23}}{L}\cot\left(\frac{\pi\xi_{23}}{L}\right)-\frac{\pi\rho_{13}}{L}\cot\left(\frac{\pi\xi_{13}}{L}\right)\right]+\cdots, \quad (3.47)$$

where the EE $S(A_1\cup A_2)$ for the mixed state $A_1\cup A_2$ is given as

$$S(A_1\cup A_2)=\frac{C_L}{6}\log\left[\frac{L}{\pi a}\sin(\frac{\pi\xi_{13}}{L})\right]+\frac{C_M}{6}\frac{\pi\rho_{13}}{L}\cot\left(\frac{\pi\xi_{13}}{L}\right)+\cdots. \quad (3.48)$$

Similar to the previous case, by the application of an appropriate adjacent limit in the disjoint intervals result given in Eq. (3.34) we may reproduce the above adjacent intervals result in Eq. (3.46). Also note that the right-hand-side of Eq. (3.47) matches with the corresponding EWCS obtained in [33] up to an additive constant which is contained in the undetermined OPE coefficient of the corresponding three point twist correlator.

3.3.3 Adjacent intervals at a finite temperature

We now proceed to the case of two adjacent intervals at a finite temperature T in a $GCFT_{1+1}$. To this end, we consider the bipartite mixed state described by $A_1\equiv[(\xi_1,\rho_1),(\xi_2,\rho_2)]$ and $A_2\equiv[(\xi_2,\rho_2),(\xi_3,\rho_3)]$ in a $GCFT_{1+1}$ defined on a thermal cylinder with the circumference given by the inverse temperature $\beta=1/T$. Similar to the previous subsection, we need to compute the three point twist correlator in Eq. (3.41) on the thermal cylinder. This is done by utilizing the map (3.36) and the transformation of $GCFT$ primaries in

Eq. (3.37) to obtain

$$\begin{aligned}&\left\langle \Phi_{n_o}(\xi_1,\rho_1)\Phi^2_{-n_o}(\xi_2,\rho_2)\Phi_{n_o}(\xi_3,\rho_3)\right\rangle_\beta\\&=\left(\frac{\beta}{2\pi}\right)^{-2h_L^{(1)}-h_L^{(2)}}\exp\left[\frac{2\pi}{\beta}(\xi_1 h_L^{(1)}+\xi_2 h_L^{(2)}+\xi_3 h_L^{(1)}\right.\\&\left.+\rho_1 h_M^{(1)}+\rho_2 h_M^{(2)}+\rho_3 h_M^{(1)})\right]\\&\times\left\langle \Phi_{n_o}(u_1)\Phi^2_{-n_o}(u_2)\Phi_{n_o}(v_2)\right\rangle.\end{aligned}\tag{3.49}$$

Here the subscript β on the left denotes that the correlator is described on the thermal cylinder and the three point twist correlator on the right-hand-side is described on the $GCFT$ complex plane. Now utilizing Eqs. (3.49) and (3.8) we may obtain the OEE for the mixed states of two adjacent intervals at a finite temperature to be

$$\begin{aligned}S_o(A_1:A_2)&=\frac{C_L}{12}\log\left[\left(\frac{\beta}{\pi a}\right)^3\sinh\left(\frac{\pi\xi_{12}}{\beta}\right)\right.\\&\left.\times\sinh\left(\frac{\pi\xi_{23}}{\beta}\right)\sinh\left(\frac{\pi\xi_{13}}{\beta}\right)\right]\\&+\frac{C_M}{12}\left[\frac{\pi\rho_{12}}{\beta}\coth\left(\frac{\pi\xi_{12}}{\beta}\right)+\frac{\pi\rho_{23}}{\beta}\coth\left(\frac{\pi\xi_{23}}{\beta}\right)\right.\\&\left.+\frac{\pi\rho_{13}}{\beta}\coth\left(\frac{\pi\xi_{13}}{\beta}\right)\right]+\cdots,\end{aligned}\tag{3.50}$$

where a is a UV cut off of the $GCFT_{1+1}$. We may again rearrange the above expression to obtain

$$\begin{aligned}&S_o(A_1:A_2)-S(A_1\cup A_2)\\&=\frac{C_L}{12}\log\left[\frac{\beta}{\pi a}\frac{\sinh\left(\frac{\pi\xi_{12}}{\beta}\right)\sinh\left(\frac{\pi\xi_{23}}{\beta}\right)}{\sinh\left(\frac{\pi\xi_{13}}{\beta}\right)}\right]\\&+\frac{C_M}{12}\left[\frac{\pi\rho_{12}}{\beta}\coth\left(\frac{\pi\xi_{12}}{\beta}\right)\right.\\&\left.+\frac{\pi\rho_{23}}{\beta}\coth\left(\frac{\pi\xi_{23}}{\beta}\right)-\frac{\pi\rho_{13}}{\beta}\coth\left(\frac{\pi\xi_{13}}{\beta}\right)\right]+\cdots,\end{aligned}\tag{3.51}$$

where the EE $S(A_1\cup A_2)$ for the subsystem $A_1\cup A_2$ is given as

$$\begin{aligned}S(A_1\cup A_2)&=\frac{C_L}{6}\log\left[\frac{\beta}{\pi a}\sinh(\frac{\pi\xi_{13}}{\beta})\right]\\&+\frac{C_M}{6}\frac{\pi\rho_{13}}{\beta}\coth\left(\frac{\pi\xi_{13}}{\beta}\right)+\cdots.\end{aligned}\tag{3.52}$$

Again we note that through the appropriate adjacent limit in the corresponding disjoint intervals result in Eq. (3.40) we may obtain the result for the OEE for the mixed state configuration of two adjacent intervals in Eq. (3.50). We also observe that the right-hand-side of Eq. (3.51) matches with the corresponding EWCS computed in the context of flat space holography in [33] apart from an additive constant which is contained in the undetermined OPE coefficient of the corresponding three point twist correlator. These serve as consistency checks for our computations.

3.4 OEE for a single interval

Having computed the OEE for the mixed states of two disjoint and two adjacent intervals, finally, in this subsection we proceed to the computation of the OEE for bipartite pure and mixed state configurations involving a single interval in $GCFT_{1+1}$s.

3.4.1 Single interval at zero temperature

For this case, we consider a single boosted interval $A_1=[(x_1,t_1),(x_2,t_2)]$ at zero temperature which describes a bipartite pure state in a $GCFT_{1+1}$. We may obtain this configuration through the limit $u_2\to v_1$ and $v_2\to u_1$ in the disjoint intervals construction described in Sect. 3.2. Here the interval $A\equiv A_1\cup A_2$ describes the full system with B as a null set and consequently the state described by the density matrix ρ_A is a pure state. In this limit the four point twist correlator in Eq. (3.11) reduces to the following two point twist correlator,

$$\mathrm{Tr}(\rho_A^{T_{A_2}})^{n_o}=\left\langle \Phi^2_{n_o}(u_1)\Phi^2_{-n_o}(v_1)\right\rangle,\tag{3.53}$$

where the twist operators $\Phi^2_{n_o}$ and $\Phi^2_{-n_o}$ have the weights $h_L^{(2)}=h_L^{(1)}$ and $h_M^{(2)}=h_M^{(1)}$. Now utilizing the usual form of a $GCFT$ two point correlator given in Eq. (3.7) for the above twist correlator, we may obtain the OEE for the given pure state of a single interval as follows

$$S_o(A_1:A_2)=\frac{C_L}{6}\log\left(\frac{t_{12}}{a}\right)+\frac{C_M}{6}\left(\frac{x_{12}}{t_{12}}\right)+\cdots,\tag{3.54}$$

where a is a UV cut-off for the $GCFT_{1+1}$. We observe here that the OEE obtained above matches exactly with the corresponding EWCS [33] and with the EE [22] for the single interval A_1. This is in conformity with the quantum information theory expectation that for a pure state the OEE should reduce to the EE for the single interval describing the bipartite state [8].

3.4.2 Single interval in a finite size system

In this subsection, we focus on the computation of the OEE for the pure state of a single interval in a finite sized $GCFT_{1+1}$. To this end, we consider a single interval A in a $GCFT_{1+1}$ defined on cylinder with circumference L. Using

Eq. (3.32) in Eq. (3.7), we may obtain the corresponding two point twist correlator on this cylinder as follows

$$\left\langle \Phi^2_{n_o}(\xi_1,\rho_1)\Phi^2_{-n_o}(\xi_2,\rho_2)\right\rangle = \left[\frac{L}{\pi}\sin\left(\frac{\pi\xi_{12}}{L}\right)\right]^{-2h_L^{(2)}} \times \exp\left[-2h_M^{(2)}\frac{\pi\rho_{12}}{L}\cot\left(\frac{\pi\xi_{12}}{L}\right)\right], \tag{3.55}$$

where $(\xi_i\,,\rho_i)$ are the endpoints of the interval A on the cylinder. Now by using Eq. (3.55) and Eqs. (2.2) and (2.3), we may obtain the OEE for the single interval in a finite sized system as

$$S_o(A_1:A_2) = \frac{C_L}{6}\log\left(\frac{L}{\pi a}\sin\frac{\pi\xi_{12}}{L}\right) + \frac{C_M}{6}\frac{\pi\rho_{12}}{L}\cot\frac{\pi\xi_{12}}{L} + \cdots . \tag{3.56}$$

We again observe the consistent behaviour of the OEE obtained above to match exactly with the EE and the EWCS for the corresponding single interval [29]. These matchings serve as a consistency checks for our result.

3.4.3 Single interval at a finite temperature

For this final case, we consider a single interval $A \equiv [(-\xi,-\rho),(0,0)]$ in a $GCFT_{1+1}$ defined on a thermal cylinder whose circumference is equal to the inverse temperature β. Similar to the relativistic case discussed in Sect. 2.4.3, it is necessary to consider the single interval in question to be sandwiched between two large but finite auxiliary intervals $B_1 \equiv [(-L,-y),(-\xi,-\rho)]$ and $B_2 \equiv [(0,0),(L,y)]$ adjacent on either side.[8] The OEE is then computed with finite auxiliary intervals and finally the bipartite limit described $B \equiv B_1 \cup B_2 \to A^c$ or $L \to \infty$ is taken to restore the original configuration.

With the presence of two auxiliary intervals, the OEE may then be obtained by computing the following four twist correlator on the thermal cylinder,

$$S_o(A:B) = \lim_{L\to\infty}\lim_{n_o\to 1}\frac{1}{1-n_o}\ln \times\left[\left\langle\Phi_{n_o}(-L,-y)\,\Phi^2_{-n_o}(-\xi,-\rho)\,\Phi^2_{n_o}(0,0)\,\Phi_{-n_o}(L,y)\right\rangle_\beta\right]. \tag{3.57}$$

[8] In [28,36], the authors found that a similar construction was required to appropriately compute the entanglement negativity and the reflected entropy for the same configuration of a single interval at a finite temperature in a $GCFT_{1+1}$.

The above four point twist correlator on a $GCFT$ complex plane is given by [28]

$$\left\langle\Phi_{n_o}(x_1,t_1)\,\Phi^2_{-n_o}(x_2,t_2)\,\Phi^2_{n_o}(x_3,t_3)\,\Phi_{-n_o}(x_4,t_4)\right\rangle = \frac{\tilde{k}_{n_o}}{t_{14}^{2h_L}t_{23}^{2h_L}}\frac{\mathcal{F}_{n_o}\left(T,\frac{X}{T}\right)}{T^{h_L}} \times\exp\left[-2h_M\frac{x_{14}}{t_{14}}-2h_M\frac{x_{23}}{t_{23}}-h_M\frac{X}{T}\right], \tag{3.58}$$

where $\tilde{k}_{n_o}$ is a constant, X and T are the $GCFT_{1+1}$ cross-ratios given in Eq. (3.10), $h_L \equiv h_L^{(1)} = h_L^{(2)}$, $h_M \equiv h_M^{(1)} = h_M^{(2)}$ and $\mathcal{F}_{n_o}$ is a non-universal function of the cross-ratios and depend on the full operator content of the theory. In the limits $T \to 1$ and $T \to 0$, the non-universal function $\mathcal{F}_{n_o}$ have the following behaviour [28]

$$\mathcal{F}_{n_o}(1,0) = 1, \quad \mathcal{F}_{n_o}\left(0,\frac{X}{T}\right) = C_{n_o}, \tag{3.59}$$

where C_{n_o} is a constant that depends on the full operator content of the theory.

We may utilize the conformal map (3.36) and transformation of the $GCFT$ primaries given in Eq. (3.37) to obtain the required four point twist correlator in Eq. (3.57) on the thermal cylinder as

$$\left\langle\Phi_{n_o}(-L,-y)\,\Phi^2_{-n_o}(-\xi,-\rho)\,\Phi^2_{n_o}(0,0)\,\Phi_{-n_o}(L,y)\right\rangle_\beta = \frac{k_{n_o}k_{n_o/2}^2}{T^{h_L}}\left[\frac{\beta}{\pi}\sinh\left(\frac{2\pi L}{\beta}\right)\right]^{-2h_L}\left[\frac{\beta}{\pi}\sinh\left(\frac{\pi\xi}{\beta}\right)\right]^{-2h_L} \times\exp\left[-\frac{2\pi y}{\beta}\coth\left(\frac{2\pi L}{\beta}\right)2h_M - \frac{2\pi\rho}{\beta}\coth\left(\frac{\pi\xi}{\beta}\right)2h_M-\frac{X}{T}h_M\right]\mathcal{F}_{n_o}\left(T,\frac{X}{T}\right). \tag{3.60}$$

Now using the above expression in Eq. (3.57) and taking the bipartite limit $L \to \infty$ subsequent to the replica limit $n_o \to 1$, we may obtain the OEE for the mixed state under consideration to be

$$\begin{aligned} S_o(A:B) = \lim_{L\to\infty}\Bigg[&\frac{C_L}{6}\log\left(\frac{\beta}{\pi a}\sinh\frac{2\pi L}{\beta}\right) + \frac{C_M}{6}\frac{\pi(2y)}{\beta}\coth\frac{2\pi L}{\beta}\Bigg] \\ &+\frac{C_L}{6}\log\left(\frac{\beta}{\pi a}\sinh\frac{\pi\xi}{\beta}\right) + \frac{C_M}{6}\frac{\pi\rho}{\beta}\coth\frac{\pi\xi}{\beta} - \frac{C_L}{6}\frac{\pi\xi}{\beta} - \frac{C_M}{6}\frac{\pi\rho}{\beta} \\ &+ f\left(e^{-\frac{2\pi\xi}{\beta}},-\frac{2\pi\rho}{\beta}\right)+\cdots, \end{aligned} \tag{3.61}$$

where a is a UV cut off and the non universal function $f(T, X/T)$ is defined as [28]

$$f\left(T, \frac{X}{T}\right) \equiv \lim_{n_o \to 1} \ln\left[\mathcal{F}_{n_o}\left(T, \frac{X}{T}\right)\right]. \tag{3.62}$$

Note that the divergent first term inside the parenthesis in Eq. (3.61) describes the EE of the total thermal system $A \cup B_1 \cup B_2$ with the bipartite limit $B = B_1 \cup B_2 \to A^c$. We may extract the finite part of the OEE for the mixed state of the single interval under consideration as

$$\begin{aligned} S_o(A:B) - S(A \cup B) &= \frac{C_L}{6} \log\left(\frac{\beta}{\pi a} \sinh \frac{\pi \xi}{\beta}\right) \\ &+ \frac{C_M}{6} \frac{\pi \rho}{\beta} \coth \frac{\pi \xi}{\beta} \\ &- \frac{\pi \xi C_L}{6\beta} - \frac{\pi \rho C_M}{6\beta} + f\left(e^{-\frac{2\pi\xi}{\beta}}, -\frac{2\pi\rho}{\beta}\right) + \cdots, \end{aligned} \tag{3.63}$$

where the divergent total entropy $S(A \cup B)$ has been subtracted. We observe that the above result may be expressed in a more instructive way as follows

$$\begin{aligned} S_o(A:B) - S(A \cup B) &= S(A) - S^{\text{th}}(A) \\ &+ f\left(e^{-\frac{2\pi\xi}{\beta}}, -\frac{2\pi\rho}{\beta}\right) + \cdots, \end{aligned} \tag{3.64}$$

where $S(A)$ denotes the EE for the single interval A [21] and $S^{\text{th}}(A)$ denotes the thermal contribution to the EE. The above expression highlights that the universal part of the OEE does not include contributions from the thermal correlations. We note here that the right-hand-side of Eq. (3.63) matches with the upper bound of the corresponding EWCS obtained in [33] apart from an additive constant. This extra additive constant in the EWCS is contained in the non-universal function $f(T, X/T)$ and may be obtained through a proper large central charge monodromy analysis of the four point twist correlator in Eq. (3.57).

4 Summary and conclusions

To summarize, in this article we have obtained the odd entanglement entropy for bipartite states in of $(1+1)$-dimensional holographic relativistic and non-relativistic (Galilean) conformal field theories through appropriate replica techniques. From our results we have verified the proposed duality of the bulk EWCS with the difference between the OEE and the EE for bipartite states in holographic CFT_{1+1} and $GCFT_{1+1}$. In this context we have demonstrated the extension of the above duality for $GCFT_{1+1}$s dual to bulk $(2+1)$-dimensional asymptotically flat geometries.

For the relativistic case we have obtained the OEE for bipartite pure and mixed states at zero and finite temperature and for finite sized system involving two disjoint, two adjacent and a single interval in CFT_{1+1}s through a replica technique. In this context we have obtained the corresponding results for the various bipartite states in relativistic CFT_{1+1} which were missing in the literature. Furthermore we have also verified the holographic duality of the difference between the OEE and the EE with the corresponding bulk EWCS for the above mentioned bipartite states. We also found that our result for the adjacent intervals at zero temperature matches with earlier works in the literature in the context of 1-dimensional harmonic spin chains and for gravitational path integral computations based on fixed area states. These serve as consistency checks for our computations.

Subsequent to the above we have investigated non-relativistic holographic $GCFT_{1+1}$s and established an appropriate replica technique to compute the OEE for bipartite states. In this context have computed the OEE for such bipartite states in $GCFT_{1+1}$s involving two disjoint, two adjacent and a single interval at zero and finite temperatures and for finite sized systems. Furthermore we have also compared our results with the corresponding bulk EWCS to verify and extend its duality with the difference between the OEE and EE to a flat holographic scenario.

In the above connection we have obtained the OEE for the mixed state configuration of two disjoint intervals at zero and a finite temperature and in a finite sized system utilizing a geometric monodromy technique to obtain the large central charge limit of the corresponding four point twist field correlator in the $GCFT_{1+1}$. Interestingly for the all the cases we observed that the difference between the OEE and the EE are exactly equal to the corresponding bulk EWCS computed earlier in the literature, which substantiates our computations and extends the duality to the framework of flat holography.

Following this we have obtained the OEE for the mixed state configuration of two adjacent intervals at zero and a finite temperature and in a finite sized system in $GCFT_{1+1}$s. As a consistency check we have also obtained the above results from the OEE for disjoint intervals through a suitable adjacent limit. Once again we have compared our results with bulk EWCS computed earlier in the literature in the context of flat holography and observed the matching with the functional form of the difference between the OEE and the EE. However we should mention here that the bulk EWCS for these cases involve an extra additive constant arising from the undetermined OPE coefficient of the corresponding three point twist correlator in the dual $GCFT_{1+1}$.

Subsequently, we consider the pure state configuration of a single interval at zero temperature and in a finite sized system. We have found that the OEE for these pure state configurations exactly match with the corresponding entanglement entropies (EE) as dictated by the quantum information theory. Finally for the mixed state of a single interval at a finite temperature in the $GCFT_{1+1}$s it was required to utilize a construction involving two large but finite auxil-

iary intervals adjacent on either sides of the single interval to correctly compute the corresponding OEE. We mention here that similar constructions have been employed in the literature for the computation of entanglement negativity and reflected entropy for this specific mixed state configuration in both relativistic and non-relativistic scenarios. Furthermore it was observed the OEE for this bipartite state involves a divergent part due the EE of the total (infinite) system. However, on subtraction of this divergent contribution from the universal part of the OEE, we observe that the finite part matches with the upper bound of the corresponding bulk EWCS computed earlier for flat space holography. Additionally, in the appendix A we have also reproduced the expression for the OEE for two disjoint intervals in a $GCFT_{1+1}$ through an appropriate non-relativistic limit of the corresponding result in the usual relativistic CFT_{1+1}. All of these detailed comparisons and matches serve as strong consistency checks for our computations.

In conclusion we state that the characterization of entanglement for bipartite states in conformal field theories and its relation with space time holography is an extremely rich field for further investigation and has provided significant insights into diverse issues in condensed matter theories and also in quantum gravity and black hole information. There are exciting open avenues in this context for further investigation of various other entanglement measures defined in quantum information theory which is expected to provide further elucidation of crucial issues in the above disciplines. We hope to return to these fascinating issues in the near future.

Data Availability Statement This manuscript has no associated data or the data will not be deposited. [Authors' comment: Note that this is a purely theoretical article and hence there is no data to be shared or deposited.]

Funded by SCOAP[3]. SCOAP[3] supports the goals of the International Year of Basic Sciences for Sustainable Development.

Appendix A: Limiting analysis

In this appendix we perform a limiting analysis and show that the OEE for a bipartite mixed state in a $GCFT_{1+1}$ computed in Sect. 3 can be obtained from the corresponding relativistic result in Sect. 2 through an appropriate non-relativistic limit. In this regard, the parametric İnönü-Wigner contraction given in Eq. (3.1) may be expressed in terms of the coordinates of the CFT_{1+1} complex plane as

$$z \to t + \epsilon x \ , \qquad \bar{z} \to t - \epsilon x \ , \tag{A.1}$$

where $\epsilon \to 0$. The central charges of the GCA_{1+1} may also be related to those of the parent relativistic theory as [20,33]

$$C_L = c + \bar{c} \quad , \quad C_M = \epsilon(c - \bar{c}) \ . \tag{A.2}$$

For unequal central charges c and $\bar{c}$ for the holomorphic and anti-holomorphic sectors, the OEE for the bipartite mixed state of two disjoint intervals in a CFT_{1+1} given in Eq. (2.9) may be expressed as

$$\begin{aligned} S_o(A_1 : A_2) = S(A_1 \cup A_2) + \frac{c}{12} \log \left[\frac{1+\sqrt{x}}{1-\sqrt{x}} \right] \\ + \frac{\bar{c}}{12} \log \left[\frac{1+\sqrt{\bar{x}}}{1-\sqrt{\bar{x}}} \right] + \cdots , \end{aligned} \tag{A.3}$$

where the entanglement entropy $S(A_1 \cup A_2)$ is similarly expressed in terms of the unequal central charges c and $\bar{c}$. Utilizing Eq. (A.1), we may write the CFT_{1+1} cross ratios $x, \bar{x}$ in terms of the $GCFT_{1+1}$ cross ratios X, T as

$$x \to T \left(1 + \epsilon \frac{X}{T} \right) \ , \qquad \bar{x} \to T \left(1 - \epsilon \frac{X}{T} \right) \ . \tag{A.4}$$

We may now obtain the OEE for the corresponding bipartite configuration in the $GCFT_{1+1}$ up to linear order in ϵ by utilizing Eqs. (A.4) and (A.1) in Eq. (A.3) to be

$$\begin{aligned} S_o(A_1 : A_2) = \frac{C_L}{6} \log \left(\frac{t_{14} t_{23}}{a^2} \right) + \frac{C_L}{12} \log \left(\frac{1+\sqrt{T}}{1-\sqrt{T}} \right) \\ + \frac{C_M}{6} \left(\frac{x_{14}}{t_{14}} + \frac{x_{23}}{t_{23}} \right) \\ + \frac{C_M}{12} \frac{X}{\sqrt{T}} \left(\frac{1}{1-T} \right) + \mathcal{O}(\epsilon). \end{aligned} \tag{A.5}$$

It is remarkable that the above expression matches exactly with the corresponding replica technique result in Eq. (3.29) up to the leading order which provides a consistency check for our computations. Similarly, we have checked that this limiting behaviour of the OEE in $GCFT_{1+1}$ also holds for the other bipartite configurations discussed in this article as well. We note here that although it is possible to obtain the expression for the OEE for bipartite subsystems in $GCFT_{1+1}$s following the above procedure, however the above limiting analysis lacks the information about the structure of the replica manifold which is important in the study of the Rényi generalization of the OEE and its application in holography.

References

1. P. Calabrese, J.L. Cardy, Entanglement entropy and quantum field theory. J. Stat. Mech. **0406**, P06002 (2004). arXiv:hep-th/0405152
2. P. Calabrese, J.L. Cardy, Evolution of entanglement entropy in one-dimensional systems. J. Stat. Mech. **0504**, P04010 (2005). arXiv:cond-mat/0503393
3. P. Calabrese, J. Cardy, Entanglement entropy and conformal field theory. J. Phys. A **42**, 504005 (2009). arXiv:0905.4013 [cond-mat.stat-mech]
4. G. Vidal, R.F. Werner, Computable measure of entanglement. Phys. Rev. A **65**, 032314 (2002). arXiv:quant-ph/0102117
5. M.B. Plenio, Logarithmic negativity: A full entanglement monotone that is not convex. Phys. Rev. Lett. **95**(9), 090503 (2005). arXiv:quant-ph/0505071
6. S. Dutta, T. Faulkner, A canonical purification for the entanglement wedge cross-section. JHEP **03**, 178 (2021). arXiv:1905.00577 [hep-th]
7. H.-S. Jeong, K.-Y. Kim, M. Nishida, Reflected entropy and entanglement wedge cross section with the first order correction. JHEP **12**, 170 (2019). arXiv:1909.02806 [hep-th]
8. K. Tamaoka, Entanglement wedge cross section from the dual density matrix. Phys. Rev. Lett. **122**(14), 141601 (2019). arXiv:1809.09109 [hep-th]
9. A. Mollabashi, K. Tamaoka, A field theory study of entanglement wedge cross section: Odd entropy. JHEP **08**, 078 (2020). arXiv:2004.04163 [hep-th]
10. Y. Kusuki, K. Tamaoka, Entanglement wedge cross section from CFT: Dynamics of local operator quench. JHEP **02**, 017 (2020). arXiv:1909.06790 [hep-th]
11. M. Ghasemi, A. Naseh, R. Pirmoradian, Odd entanglement entropy and logarithmic negativity for thermofield double states,. arXiv:2106.15451 [hep-th]
12. J. Angel-Ramelli, C. Berthiere, V.G.M. Puletti, L. Thorlacius, Logarithmic negativity in quantum Lifshitz theories. JHEP **09**, 011 (2020). arXiv:2002.05713 [hep-th]
13. C. Berthiere, H. Chen, Y. Liu, B. Chen, Topological reflected entropy in Chern-Simons theories. Phys. Rev. B **103**(3), 035149 (2021). arXiv:2008.07950 [hep-th]
14. X. Dong, X.-L. Qi, M. Walter, Holographic entanglement negativity and replica symmetry breaking. JHEP **06**, 024 (2021). arXiv:2101.11029 [hep-th]
15. T. Takayanagi, K. Umemoto, Entanglement of purification through holographic duality. Nat. Phys. **14**(6), 573–577 (2018). arXiv:1708.09393 [hep-th]
16. C. Akers, T. Faulkner, S. Lin, P. Rath, Reflected entropy in random tensor networks. arXiv:2112.09122 [hep-th]
17. Q. Wen, Balanced partial entanglement and the entanglement wedge cross section. JHEP **04**, 301 (2021). arXiv:2103.00415 [hep-th]
18. A. Bagchi, I. Mandal, On representations and correlation functions of galilean conformal algebras. Phys. Lett. B **675**, 393–397 (2009). arXiv:0903.4524 [hep-th]
19. A. Bagchi, R. Gopakumar, Galilean conformal algebras and AdS/CFT. JHEP **07**, 037 (2009). arXiv:0902.1385 [hep-th]
20. A. Bagchi, R. Gopakumar, I. Mandal, A. Miwa, GCA in 2d. JHEP **08**, 004 (2010). arXiv:0912.1090 [hep-th]
21. A. Bagchi, R. Basu, D. Grumiller, M. Riegler, Entanglement entropy in Galilean conformal field theories and flat holography. Phys. Rev. Lett. **114**(11), 111602 (2015). arXiv:1410.4089 [hep-th]
22. R. Basu, M. Riegler, Wilson lines and holographic entanglement entropy in galilean conformal field theories. Phys. Rev. D **93**(4), 045003 (2016). arXiv:1511.08662 [hep-th]
23. H. Jiang, W. Song, Q. Wen, Entanglement entropy in flat holography. JHEP **07**, 142 (2017). arXiv:1706.07552 [hep-th]
24. E. Hijano, C. Rabideau, Holographic entanglement and Poincaré blocks in three-dimensional flat space. JHEP **05**, 068 (2018). arXiv:1712.07131 [hep-th]
25. V. Godet, C. Marteau, Gravitation in flat spacetime from entanglement. JHEP **12**, 057 (2019). arXiv:1908.02044 [hep-th]
26. A. Bagchi, Correspondence between asymptotically flat spacetimes and nonrelativistic conformal field theories. Phys. Rev. Lett. **105**, 171601 (2010). arXiv:1006.3354 [hep-th]
27. A. Bagchi, R. Basu, 3D flat holography: Entropy and logarithmic corrections. JHEP **03**, 020 (2014). arXiv:1312.5748 [hep-th]
28. V. Malvimat, H. Parihar, B. Paul, G. Sengupta, Entanglement negativity in Galilean conformal field theories. Phys. Rev. D **100**(2), 026001 (2019). arXiv:1810.08162 [hep-th]
29. D. Basu, A. Chandra, H. Parihar, G. Sengupta, Entanglement negativity in flat holography. SciPost Phys. **12**, 074 (2022). arXiv:2102.05685 [hep-th]
30. P. Chaturvedi, V. Malvimat, G. Sengupta, Holographic quantum entanglement negativity. JHEP **05**, 172 (2018). arXiv:1609.06609 [hep-th]
31. P. Jain, V. Malvimat, S. Mondal, G. Sengupta, Holographic entanglement negativity conjecture for adjacent intervals in AdS_3/CFT_2. Phys. Lett. B **793**, 104–109 (2019). arXiv:1707.08293 [hep-th]
32. V. Malvimat, S. Mondal, B. Paul, G. Sengupta, Holographic entanglement negativity for disjoint intervals in AdS_3/CFT_2. Eur. Phys. J. C **79**(3), 191 (2019). arXiv:1810.08015 [hep-th]
33. D. Basu, A. Chandra, V. Raj, G. Sengupta, Entanglement wedge in flat holography and entanglement negativity. SciPost Phys. Core **5**, 013 (2022). arXiv:2106.14896 [hep-th]
34. H. A. Camargo, P. Nandy, Q. Wen, H. Zhong, Balanced partial entanglement and mixed state correlations. arXiv:2201.13362 [hep-th]
35. D. Basu, Balanced partial entanglement in flat holography. arXiv:2203.05491 [hep-th]
36. J. K. Basak, H. Chourasiya, V. Raj, G. Sengupta, Reflected entropy in Galilean conformal field theories and flat holography. arXiv:2202.01201 [hep-th]
37. M. R. Setare, M. Koohgard, The reflected entropy in the GMMG/GCFT flat holography. arXiv:2201.11741 [hep-th]
38. E. Hijano, Semi-classical BMS_3 blocks and flat holography. JHEP **10**, 044 (2018). arXiv:1805.00949 [hep-th]
39. P. Calabrese, J. Cardy, E. Tonni, Entanglement negativity in extended systems: A field theoretical approach. J. Stat. Mech. **1302**, P02008 (2013). arXiv:1210.5359 [cond-mat.stat-mech]
40. A.L. Fitzpatrick, J. Kaplan, M.T. Walters, Universality of long-distance AdS physics from the CFT bootstrap. JHEP **08**, 145 (2014). arXiv:1403.6829 [hep-th]
41. J. Kudler-Flam, S. Ryu, Entanglement negativity and minimal entanglement wedge cross sections in holographic theories. Phys. Rev. D **99**(10), 106014 (2019). arXiv:1808.00446 [hep-th]
42. P. Calabrese, J. Cardy, E. Tonni, Finite temperature entanglement negativity in conformal field theory. J. Phys. A **48**(1), 015006 (2015). arXiv:1408.3043 [cond-mat.stat-mech]
43. D. Basu, H. Parihar, V. Raj, G. Sengupta, Entanglement negativity, reflected entropy and anomalous gravitation. arXiv:2202.00683 [hep-th]
44. J. Kumar Basak, V. Malvimat, H. Parihar, B. Paul, G. Sengupta, On minimal entanglement wedge cross section for holographic entanglement negativity. arXiv:2002.10272 [hep-th]